POLITECNICO DI TORINO
Repository ISTITUZIONALE

New 3-D zig zag theories: elastostatic assessment of strategies differently accounting for layerwise effects of laminated and sandwich composites

Original
New 3-D zig zag theories: elastostatic assessment of strategies differently accounting for layerwise effects of laminated and sandwich composites / Urraci, Andrea; Icardi, Ugo. - In: INTERNATIONAL JOURNAL OF ENGINEERING RESEARCH AND APPLICATIONS. - ISSN 2248-9622. - ELETTRONICO. - 9:7(2019), pp. 1-25. [10.9790/9622-0907050125]

Availability:
This version is available at: 11583/2749202 since: 2019-09-02T12:51:47Z

Publisher:
IJERA Publication

Published
DOI:10.9790/9622- 0907050125

Terms of use:

This article is made available under terms and conditions as specified in the corresponding bibliographic description in the repository

Publisher copyright
default_article_editorial [DA NON USARE]

-

(Article begins on next page)

12 October 2024

RESEARCH ARTICLE OPEN ACCESS

New 3-D zig-zag theories: elastostatic assessment of strategies differently accounting for layerwise effects of laminated and sandwich composites

Andrea Urraci*, Ugo Icardi**
**(Dipartimento di Ingegneria Meccanica e Aerospaziale, Politecnico di Torino, Italy)*
*** (Dipartimento di Ingegneria Meccanica e Aerospaziale, Politecnico di Torino, Italy)*
Corresponding Author : Andrea Urraci

ABSTRACT
New physically based 3-D, fixed d.o.f., theories which enable to analyze cases with general loading and boundary conditions efficiently are proposed. Here the aim is to study the effects of an arbitrary choice of through-thickness representation of kinematic/stress variables and of zig-zag functions. The same trial functions and expansion order of analytical solutions are assumed to assess theories under the same conditions. Comparisons are carried out with exact and/or 3-D FEA solutions. Their computational burden is still comparable to that of classical plate models. The results show that whenever coefficients of representation are recalculated across the thickness by enforcing the fulfillment of all constraints prescribed by the elasticity theory, the choice of the representation form and of zig-zag functions is immaterial. In this way, a high order of generalization is allowed because the representation of one single displacement can be freely varied across the thickness and be completely different from that of other displacements. Moreover, zig-zag functions can be arbitrarily chosen or even omitted without any accuracy loss. Instead, accuracy is shown to be strongly dependent upon the assumptions made for theories only partially satisfying constraints.
Keywords - Composite and sandwich plates, zig-zag theories, interlaminar transverse shear/normal stress continuity, localized and distributed loadings, FEA 3-D elastostatic solutions

---

Date Of Submission: 30-06-2019 Date Of Acceptance: 20-07-2019

I. INTRODUCTION

Owing to their excellent specific properties, nowadays laminated and sandwich composites are widely used to build primary structures in many engineering fields, such as aerospace, naval and terrestrial applications.

Anyway, their entirely different and more complex behaviour than metals requires a more sophisticate modeling. Characteristic feature, their displacement field must be C°-continuous (zig-zag effect) in order to fulfill out-of-plane stresses continuity across the thickness necessary for equilibrium.

So far, many theories with very different characteristics, accuracy and computational cost have been created for analysis of laminated and sandwich composites. The papers by Carrera and co-workers [1]-[5], Demasi [6], Vasilive and Lur'e [7], Reddy and Robbins [8], Lur'e, and Shumova [9], Noor et al. [10], Altenbach [11], Khandan et al. [12] and Kapuria and Nath [13] and the book by Reddy [14] are cited as examples wherein a broad discussion of this matter can be found. But many others with the same characteristics are available in the literature, which is outside the purpose of this paper to quote. As universally accepted, sandwiches are described as multilayered structures made of one or more tick and compliant layers as the core/cores and stiff and relatively thinner layers as the faces, whenever cell-scale effects are disregarded.

In a broad outline the analysis of laminated and sandwich structures can be carried out using equivalent single-layer (ESL), discrete-layer (DL) and zig-zag (ZZ) theories, which further subdivide into displacement-based and mixed theories, depending on if strains and stresses are obtained from constitutive relations or are chosen separately from each other, within the framework of Hellinger-Reissner (HR) or Hu-Washizu (HW) variational theorems. As is well known, ESL completely disregard layerwise effects, therefore are only suitable for an overall response analysis, but cases exist for which they are not valid even for this purpose (see, e.g. e.g. [15] to [25]). Certainly these theories cannot be used successfully for sandwich analysis, as they cannot account for the strong layerwise effects due to the very different properties of core and faces that also affect the global behaviour. Layerwise theories further subdivide into discrete-layer (DL) and zig-zag (ZZ) theories (acronyms used throughout the paper are defined in Table 1). As DL assume variables and description

apart for each layer, they could overwhelm the computational capacity when structures of industrial interest are analyzed, but anyway they are still the most accurate theories, irrespective for lay-up, layer properties, loading and boundary conditions.

ZZ theories to date collect an increasing interest because they strike the right balance between accuracy and cost saving, so meeting designers' demand of theories in a simple already accurate form. These theories can be further subdivided into physically-based (DZZ) and kinematic-based (MZZ) zig-zag theories. Layerwise contributions of ZZ are embodied as the product of linear [26] or nonlinear [27] zig-zag functions and unknown zig-zag amplitudes which are determined through the enforcement of interfacial stress compatibility conditions. In DZZ, generally but still not always stresses derive from kinematics and stress-strain relations, but mixed formulations are also known for these theories.

In MZZ, no amplitude is incorporated which must be pre-calculated, since zig-zag functions are a priori assumed to feature a periodic change of the slope of displacements at interfaces, which, strictly speaking, occurs only for periodic lay-ups. Stresses of MZZ are assumed apart from kinematics, so they constitute mixed theories. Because their layerwise functions are insensitive to the physical characteristics of the lamination and their kinematics is usually assumed in a simplified form, MZZ can accurately predict stress fields but not always displacements [28] unless a high order of expansion of solutions (i.e., larger than for DZZ) is assumed.

Carrera Unified Formulation (CUF)) [3], to date extensively used since it allows displacements to take arbitrary forms that can be chosen by the user as an input and therefore allows to study general loading and boundary conditions, does not enforce physical constraints to define layerwise functions, so it gets existing ESL and MZZ as particularizations. However also refined DZZ [13-15,17,22,23,27] have shown a comparable degree of generality and flexibility of use compared to CUF, resulting even more efficient because DZZ with coefficients redefined across each physical or computational layer [15-17] (and for this reason they are referred as adaptive theories) allow the same accuracy of CUF with fewer variables and have characteristics of generality and flexibility similar to CUF. Although they have just five fixed d.o.f. like classical plate theories, they are able to satisfy all physical and elasticity constraints, so they deserve to be tested more extensively than in [15-17] considering further challenging cases like ones already studied by the users of CUF. Moreover it must be investigated whether and which others further generalizations of DZZ can be achieved. At the present state of research, DZZ [15-17] have taken on similar characteristics to theories with a hierarchical set of locally defined polynomials (see, Catapano et al. [29] and de Miguel et al. [30]), but it remains to be further investigated whether the presence of the zigzag functions, which are computationally the most burdensome, can be eliminated through the simple redefinition of a certain coefficients of the representation, so to further improve efficiency. In this context, forms of representation within DZZ different for each displacement and with zig-zag functions completely different from those usually considered so far, or even omitting them must also be tested in order to ascertain whether the superior generality that would be achieved allows accuracy to be preserved. These evolved DZZ theories would come to assume characteristics in some ways similar to those of global-local superposition theories, see Zhen and Wanji, e.g. [22,31], representing at the same time a development that also considers the piecewise through-thickness variation of the transverse displacement. All theories of the present study take into account the transverse normal deformability, because [15-17,32,33], along many others in literature, demonstrate that inaccurate results are otherwise obtained.

A more in-depth study of this matter is presented in this paper, also through the development of new DZZ theories. The intended aim of this study is to show that: (i) a very accurate description of transverse normal deformability is required for different loading conditions; (ii) which is the minimum order of representation that is required to obtain accurate results for static cases; (iii) if theories with different functions used to represent variation across the thickness and without zig-zag functions can be as accurate as other higher-order theories. (iv) Moreover, it will be investigated the effects of only partial assumptions of zig-zag functions on accuracy. (v) Finally, another goal of this paper is to investigate extensively whether the choice of zig-zag functions is immaterial and when these functions can even be omitted without any loss of accuracy. It will also be examined whether is not necessary to assign a specific role a priori to the coefficients of displacement field if all physical constraints (compatibility of displacements and stresses, boundary conditions, imposition of equilibrium at some points across the thickness) are satisfied. Instead, it should be noticed that all these aspects and choices are very important for lower-order theories that impose only a partial satisfaction of them. Geometry, loading and boundary conditions of the cases examined in the numerical applications are reported in Table 2a, normalizations and trial functions in Table 2b and mechanical properties in Table 3.

II. THEORETICAL FRAMEWORK

For clarity, first the notations and the basic assumptions used, as well as the solution methodology, which are common to all the theories, are defined.

2.1 Notations, basic assumptions and solution methodology

A rectangular right-handed Cartesian coordinate reference system (x, y, z), whose origin is on one edge and which is on the middle reference plane Ω of the multilayered plate, is assumed as reference frame. As customary, z is assumed as the thickness coordinate ($z \in [-h/2; h/2]$ h being the overall thickness and Lx and Ly as the plate side-lengths). The constituent layers are assumed to have a uniform thickness h^k and to be made of materials with linear elastic properties and to be perfectly bonded to each other. The coordinates just after or before an interface k are indicated as ${}^{(k)}z^{+}$ and ${}^{(k)}z^{-}$, respectively, while subscripts $_k$ and superscripts ^{k} indicate belonging of quantities to the layer k and ^{u} and $_l$ are used for the upper and lower faces of the laminate. In-plane and transverse displacements components are indicated as u_α and u_ς and a comma is used to indicate spatial derivatives (e.g., $(.)_{,x} = \partial/\partial x$, $(.)_{,z} = \partial/\partial z$). To be concise, tensor notation is used throughout the paper, so in certain parts of it symbols x, y, z are replaced by Greek letters (e.g. $\alpha = 1, 2 \equiv x, y$; $\varsigma = 3 \equiv z$).

Strains, which are assumed infinitesimal, and elastic stresses are symbolized by ε_{ij} and σ_{ij}, respectively. Middle-plane displacements u^0, v^0, w^0 and the rotations of the normal $\theta_x = \Gamma_x^0(x,y) - w^0(x,y)_{,x}$, $\theta_y = \Gamma_y^0(x,y) - w^0(x,y)_{,y}$ are assumed as the only functional d.o.f. of all theories. In tensor notation is $u_\alpha^0 \equiv u^0$ if $\alpha = 1$, $u_\alpha^0 \equiv v^0$ if $\alpha = 2$. Their governing equations will not be reported in order to be concise and because they can be obtained in a straightforward way with standard techniques, which in this paper are automatically implemented using a symbolic calculus package. Only displacement, strain and stress fields will be discussed into details along with their distinctive features and how they reflect on accuracy.

Static governing equation of each theory are solved in analytical form using Rayleigh-Ritz method, given the simple geometry of the cases examined and the conservative loadings. According, each functional degree of freedom (d.o.f.) is expressed as a truncated series expansion of unknown amplitudes A_Δ^i and trial functions $\Re^i(x,y)$, which individually satisfy prescribed boundary conditions:

$$\Delta = \sum_{i=1}^{m_\Delta} A_\Delta^i \, \Re^i(x,y) \tag{1}$$

while mechanical boundary conditions (if necessary but not for the present cases) are satisfied using Lagrange multipliers method. Herein the symbol Δ represent in turns u^0, v^0, w^0, θ_x, θ_y. Amplitudes are determined solving the linear algebraic system that follows applying Rayleigh-Ritz method, namely by deriving the total potential energy functional expression with respect to unknown ones and equating to zero. Table 2b defines trial functions, expansion order and normalizations used in the numerical applications.

Regarding simply-supported edges, the following boundary conditions have to be imposed:

$$w^0(0,y) = 0 \; ; \; w^0(L_x,y) = 0 \; ; \; w^0(0,y)_{,xx} = 0 \; ; \; w^0(L_x,y)_{,xx} = 0 \tag{2}$$

$$w^0(x,0) = 0 \; ; \; w^0(x,L_y) = 0 \; ; \; w^0(x,0)_{,yy} = 0 \; ; \; w^0(x,L_y)_{,yy} = 0 \tag{3}$$

on the reference mid-plane. The boundary conditions for cylindrical bending follows in a straightforward way from (2) and (3) assuming no variations to occur in the y, (x, z) being the bending plane.

The following boundary conditions are enforced on the reference mid-surface at the clamped edge of propped-cantilever beams, which is here assumed at $x = 0$:

$$u^0(0,0) = 0 \; ; w^0(0,0) = 0 \; ; w^0(0,0)_{,x} = 0 \; ; \; \Gamma_x^0(0,0) = 0 \tag{4}$$

The following further boundary conditions are enforced in order to simulate that (4) holds identically across the thickness:

$$u_\alpha(0,z)_{,z} = 0 \; ; u_\varsigma(0,z)_{,z} = 0 \; ; u_\varsigma(0,z)_{,xz} = 0 \tag{5}$$

The following further mechanical boundary condition

$$\int_{-h/2}^{h/2} \sigma_{xz}(0,z)dz = T \tag{6}$$

is enforced to ensure that the transverse shear stress resultant force equals the constraint force at the clamped edge.

The additional support condition $w^0(L,-h/2)=0$ holds at x=L on the lower face $z=-h/2$, while condition (4) is reformulated as: $\int_{-h/2}^{h/2}\sigma_{xz}(L,z)\,dz=T_L$, for propped-cantilever beams. As mentioned above, the latter mechanical boundary conditions are enforced using Lagrange multipliers method.

Discontinuous loading distributions are studied as a a general function $\chi(x,y)$ acting on upper and/or lower faces, or just on a part of them, without being necessary using a series expansion with a very large number of components, as customary, because symbolic calculus computes exactly energy contributions, whatever form $\chi(x,y)$ takes. As a result, the structural model is made simpler to use and at the same made more accurate.

2.2 ZZA displacement-based theory

The first adaptive DZZ discussed here is ZZA zig-zag theory developed in [15], as it constitutes the basis from which all recently published theories by the authors have been obtained as its particularizations or generalizations. ZZA postulates the following displacement field across the thickness:

$$u_\alpha(x,y,z)=\left[\ u^0(x,y)+z(\Gamma^0_\alpha(x,y)-w^0(x,y)_{,\alpha})\ \right]_0+$$
$$+\left[\ F^u_\alpha(z)\ \right]_i+\left[\ \sum_{k=1}^{n_i}\Phi^k_\alpha(x,y)(z-z_k)H_k(z)+\right.$$
$$\left.+\sum_{k=1}^{n_3}{}_\alpha C^k_u(x,y)H_k(z)\ \right]_c$$

$$u_\varsigma(x,y,z)=\left[\ w^0(x,y)\ \right]_0+\left[\ F^\zeta(z)\ \right]_i$$
$$+\left[\ \sum_{k=1}^{n_i}\Psi^k(x,y)(z-z_k)H_k(z)+\right.$$
$$\left.\sum_{k=1}^{n_i}\Omega^k(x,y)(z-z_k)^2H_k(z)+\sum_{k=1}^{n_3}C^k_\varsigma(x,y)H_k(z)\ \right]_c \tag{7}$$

Contributions are subdivided into linear- $[\ldots]_0$, higher- $[\ldots]_i$ and layerwise $[\ldots]_c$ ones. The first contains only five functional degrees of freedom, while $[\ldots]_i$ can contain any combination of independent functions $\left[\ F^u_\alpha(z)\ \right]_i$ and $\left[\ F^\zeta(z)\ \right]_i$, which are chosen as:

$$\left[\ F^u_\alpha(z)\ \right]_i=\left[\ C^i_\alpha(x,y)z^2+D^i_\alpha(x,y)z^3+(Oz^4\ldots)\ \right]_i$$
$$=\left[\ {}_3(.)^{\sim}_\alpha\ \right]_i+\left[\ (Oz^4\ldots)\ \right]_i$$

$$\left[\ F^\zeta(z)\ \right]_i=\left[\ b^i(x,y)z+c^i(x,y)z^2+d^i(x,y)z^3+\right.$$
$$\left.+e^i(x,y)z^4+(Oz^5\ldots)\ \right]_i=$$
$$=\left[\ {}_4(.)^{\sim}_\zeta\ \right]_i+\left[\ (Oz^5\ldots)\ \right]_i$$

(8)

to admit [27] as a particularization, since contributions $\left[\ {}_3(.)^{\sim}_\alpha\ \right]_i$, $\left[\ {}_4(.)^{\sim}_\zeta\ \right]_i$ are the same as in this former theory, while higher-order contributions $\left[\ (Oz^4\ldots)\ \right]_i$, $+\left[\ (Oz^5\ldots)\ \right]_i$ are characteristic of ZZA. Expressions of C^i_α, D^i_α, b^i to e^i are obtained once and for all using symbolic calculus by enforcing the fulfilment of stress boundary conditions

$$\sigma_{\alpha\varsigma}=\sigma_{\varsigma\varsigma,\varsigma}=0;\sigma_{\varsigma\varsigma}=p^0(\pm) \tag{9}$$

p^0 being the distributed loading acting on upper (+) and lower (-) faces (but also non-homogeneous conditions $\sigma_{\alpha\varsigma};\ \sigma_{\beta\varsigma}\neq 0$ could be enforced without difficulty). Contributions $[\ldots]_i$ by (8) can be rearranged as:

$$U^i_\alpha(x,y,z)=[A_{\alpha2}z^2+A_{\alpha3}z^3]+A_{\alpha4}z^4+\ldots+A_{\alpha n}z^n$$
$$U^i_\zeta(x,y,z)=[A_{\varsigma1}z+A_{\varsigma2}z^2+A_{\varsigma3}z^3+A_{\varsigma4}z^4]+$$
$$+A_{\varsigma5}z^5+\ldots+A_{\varsigma n}z^n \tag{10}$$

Terms under square brackets are calculated by imposing the fulfilment of local equilibrium equations at different points across the thickness:

$$\sigma_{\alpha\beta,\beta}+\sigma_{\alpha\varsigma,\varsigma}=b_\alpha;\sigma_{\alpha\varsigma,\alpha}+\sigma_{\varsigma\varsigma,\varsigma}=b_\varsigma \tag{11}$$

It should be noticed that the in-plane position of equilibrium points must be chosen appropriately depending on boundary conditions, so to avoid null contributions. It is also important to note that coefficients are redefined across the thickness because of the imposition of (11) in different points of the thickness. Although any order of representation could be assumed, maximum accuracy is already achieved in all cases tested to date choosing a piecewise cubic representation for in-plane displacements $u^{(3)}_\alpha$ and a fourth-order one $u^{(4)}_\varsigma$ for the transverse displacement, as shown in [16,17,27]. This paper will demonstrate that in-plane and out-of-plane orders can also be exchanged into $u^{(4)}_\alpha$, $u^{(3)}_\varsigma$ without any accuracy loss. Any single constituent layer could be divided into one or more mathematical ones, with the intended aim to rising accuracy without increasing the number of d.o.f., but

this has not proved necessary in applications. The symbols n_i and $n_{\mathfrak{I}}$ in (7) represent the number of physical and mathematical layer interfaces, respectively.

Finally, layerwise contributions are included into $[...]_c$, whose amplitudes Φ_α^k, Ψ^k and Ω^k are calculated once and for all by imposing the continuity of out-of-plane stresses and of the transverse normal stress gradient $\sigma_{\varsigma\varsigma,\varsigma}$ at layer interfaces:

$$\sigma_{\alpha\varsigma}({}^{(k)}z^+) = \sigma_{\alpha\varsigma}({}^{(k)}z^-);\ \sigma_{\varsigma\varsigma}({}^{(k)}z^+) = \sigma_{\varsigma\varsigma}({}^{(k)}z^-);$$
$$\sigma_{\varsigma\varsigma,\varsigma}({}^{(k)}z^+) = \sigma_{\varsigma\varsigma,\varsigma}({}^{(k)}z^-) \qquad (12)$$

The expressions of C_u^k and C_ς^k are obtained by imposing the continuity of displacements

$$u_\alpha({}^{(k)}z^+) = u_\alpha({}^{(k)}z^-);\ u_\varsigma({}^{(k)}z^+) = u_\varsigma({}^{(k)}z^-) \qquad (13)$$

which become necessary whenever order and form of the representation are changed across the thickness, as will be done in this paper. Conditions (9, 11-13) are imposed using a symbolic calculus tool which determines once and for all the expressions of amplitudes. So assuming arbitrarily the form of representation, namely otherwise than in (7), is not a difficulty for the user, the necessary calculations being carried out automatically. In this way, DZZ can be generalized up to the level of best kinematic-based theories currently available. The choices then come to be determined only by performance considerations and not by operational opportunity.

Note that, only a small fraction of the overall processing time is required for calculating layerwise contributions because symbolic calculus provide once and for all their expressions in a closed form.

In this way, the overall processing time remains still comparable with that of ESL (see, Table 4). If just the material properties and/or the orientation of layers change, but not their number, symbolic expressions representing the solution remain the same. SEUPT technique described in [15] can be used to obtain a C° formulation of the ZZA and the other theories of this paper.

2.3 ZZA* displacement-based theory

This adaptive theory, which is a modified version of ZZA, is retaken from [16] where it was developed by replacing zig-zag layerwise functions $[...]_c$ with a power series with amplitudes to be re-determined across the thickness. ZZA* and HWZZM developed in [17] assuming arbitrary zig-zag functions are re-proposed here in order to demonstrate that layerwise contributions can be arbitrarily assumed or even omitted, whenever the full set of physical constraints (9, 11-13) is imposed. Note that the present new theories constitute evolutions of ZZA* and HWZZM based on different forms of representation. Their aim is to generalize ZZA and to obtain a reduction of the computational burden while preserving unchanged the accuracy. The following displacement field is postulated in ZZA*:

$$\begin{aligned} u_\alpha(x,y,z) = {} & [\ u^0(x,y) + z(\Gamma_\alpha^0(x,y) - w^0(x,y)_{,\alpha})\ ]_0 \\ & + \{ \sum_{k=1}^{n_{\mathfrak{I}}} {}_k\tilde{B}_\alpha^i(x,y)z + [C_\alpha^i(x,y)z^2] + \\ & + [D_\alpha^i(x,y)z^3 + D_\alpha^i(x,y)z_j^3] + \sum_{k=1}^{n_i} {}_k\tilde{C}_\alpha^i(x,y)\ \}_{i+c} \\ u_\varsigma(x,y,z) = {} & [\ w^0(x,y)\ ]_0 + \{\ [b^i(x,y)z + \sum_{k=1}^{n_{\mathfrak{I}}} {}_k\tilde{b}^i(x,y)z] + \\ & + [c^i(x,y)z^2 + \sum_{k=1}^{n_i} {}_k\tilde{c}^i(x,y)z^2] + [d^i(x,y)z^3] + \\ & + e^i(x,y)z^4 + \sum_{k=1}^{n_i} {}_k\tilde{d}^i(x,y)\ \}_{i+c} \end{aligned} \qquad (14)$$

The linear contribution is the same of ZZA, while terms ${}_k\tilde{B}_\alpha^i$, C_α^i, ${}_k\tilde{C}_\alpha^i$, ${}_k\tilde{b}^i$ and ${}_k\tilde{c}^i$ are obtained by imposing (12), (13) at interfaces between layers. Contributions C_α^i, D_α^i, b^i, c^i, d^i and e^i still allow the fulfillment of stress boundary conditions (9) and of local equilibrium equations (11). Note that b^i and c^i exist only at the first layer, while then they are assumed to vanish in the subsequent layers.

2.4 HWZZ mixed theory

HWZZ adaptive theory [17] is a mixed HW version of ZZA which is obtained preserving only essential contributions of displacement, strain and stress fields by ZZA. It is based on the following assumptions: no decomposition into mathematical layer is allowed, so C_u^k, C_v^k, C_w^k are omitted and also Ω^k are neglected, being essential only for stress fields:

$$u_\alpha(x,y,z)=[\ u^0(x,y)+z(\Gamma_x^0(x,y)-w^0(x,y)_{,\alpha})\ ]_0+$$
$$+[\ C_\alpha^i(x,y)z^2+D_\alpha^i(x,y)z^3\ ]_i+$$
$$+[\ \sum_{k=1}^{n_i}\Phi_\alpha^k(x,y)(z-z_k)H_k(z)\ ]_c$$

$$u_\varsigma(x,y,z)=[\ w^0(x,y)\ ]_0+[\ b^i(x,y)z+c^i(x,y)z^2+$$
$$+d^i(x,y)z^3+e^i(x,y)z^4\ ]_i+$$
$$[\ \sum_{k=1}^{n_i}\Psi^k(x,y)(z-z_k)H_k(z)\ ]_c \tag{15}$$

In-plane strains are obtained from the previous displacement field, while out-of-plain ones ε_{zz}, γ_{xz}, γ_{yz} are obtained from:

$$^{\Im}u_\alpha(x,y,z)=[\ u^0(x,y)+z(\Gamma_x^0(x,y)-w^0(x,y)_{,\alpha})\ ]_0+$$
$$+[\ C_\alpha^i(x,y)z^2+D_\alpha^i(x,y)z^3\ ]_i+$$
$$+[\ \sum_{k=1}^{n_i}\Phi_\alpha^k(x,y)(z-z_k)H_k(z)+\sum_{k=1}^{\Im}{}_\alpha C_u^k(x,y)H_k\ ]_c$$

$$^{\Im}w_\varsigma(x,y,z)=[\ w^0(x,y)\ ]_0+[\ b^i(x,y)z+c^i(x,y)z^2+d^i(x,y)z^3$$
$$+e^i(x,y)z^4\ ]_i+[\ \sum_{k=1}^{n_i}\Psi^k(x,y)(z-z_k)H_k(z)$$
$$+\sum_{k=1}^{\Im}C_w^k(x,y)H_k\ ]_c \tag{16}$$

In-plane stresses are calculated using stress-strain relations, while out-of-plane ones are obtained by integration of equilibrium equations.

2.5 HWZZM mixed theory

This adaptive theory [16] is a modified version of HWZZ obtained assuming different zig-zag functions, which allows to demonstrate that indistinguishable results are obtained whenever (9, 11-13) are imposed. It is developed assuming Murakami's zig-zag function $M^k(z)=(-1)^k\zeta^k$, where $\zeta^k=a^kz-b^k$, $a^k=\dfrac{2}{z_{k+1}-z_k}$, $b^k=\dfrac{z_{k+1}+z_k}{z_{k+1}-z_k}$ as the layerwise functions. The displacement field is postulated as:

$$^{\Im}u_\alpha(x,y,z)=[\ u^0(x,y)+z(\Gamma_\alpha^0(x,y)-w^0(x,y)_{,\alpha})\ ]_0+$$
$$+[\ F_\alpha^u(z)\ ]_i+[\ A_k^{u_\alpha}(z)[\frac{2z}{z_{k+1}-z_k}+$$
$$-\frac{z_{k+1}+z_k}{z_{k+1}-z_k}\ ]+C_\alpha^k(x,y)]_c$$

$$^{\Im}u_\varsigma(x,y,z)=[\ w^0(x,y)\ ]_0+[\ F^\varsigma(z)\ ]_i+[A_k^{u_\varsigma}(z)[\frac{2z}{z_{k+1}-z_k}+$$
$$-\frac{z_{k+1}+z_k}{z_{k+1}-z_k}]+B_k^{u_\varsigma}(z)[\frac{(2z)^2}{z_{k+1}-z_k}]+C_\varsigma^k(x,y)]_c \tag{17}$$

Note that here zig-zag amplitudes $A_k^{u_\varsigma}$ and $B_k^{u_\varsigma}$ are calculated by imposing the fulfillment of (12), while C_α^k and C_ς^k are obtained by imposing (13). Similarly to HWZZ, no decomposition into mathematical layer is allowed for displacement field from which in-plane strains are obtained, while out-of-plane ones are calculated restoring their subdivision. Again σ_{xx}, σ_{yy}, σ_{xy} are obtained from stress-strain relations, while σ_{xz}, σ_{yz}, σ_{zz} are calculated by integration of (11).

2.6 HWZZM* mixed theory

Another HW adaptive mixed theory was developed in [16] starting from ZZA* and assuming all the same steps needed to obtain HWZZ from ZZA. HWZZM* is retaken in this paper so to have a theory to use for comparisons in the numerical applications which is in mixed form and does not consider explicitly zig-zag contributions. The displacement field is postulated as:

$$u_\alpha(x,y,z)=[\ u^0(x,y)+z(\Gamma_\alpha^0(x,y)-w^0(x,y)_{,\alpha})\ ]_0+$$
$$+\{\ \sum_{k=1}^{n_\Im}{}_k\tilde{B}_\alpha^i(x,y)z\ \}_c+$$
$$+\{\ [C_\alpha^i(x,y)z^2]+[D_\alpha^i(x,y)z^3]\ \}_i$$

$$u_\varsigma(x,y,z)=[\ w^0(x,y)\ ]_0+\{\ [b^i(x,y)z]+[c^i(x,y)z^2]+$$
$$+[d^i(x,y)z^3]+e^i(x,y)z^4\ \}_i+$$
$$+\{\ \sum_{k=1}^{n_\Im}{}_k\tilde{b}^i(x,y)z\ \}_c \tag{18}$$

Again, no decomposition into mathematical layers is allowed for displacements, so similarly to HWZZ terms ${}_k\tilde{c}^i$, ${}_k\tilde{C}_\alpha^i$, ${}_k\tilde{d}^i$ by ZZA are omitted. In-plane strains are obtained from (18), while similarly to HWZZ, their out-of-plane counterparts are obtained admitting decomposition into

computational layers. In-plane stresses σ_{xx}, σ_{yy}, σ_{xy} are obtained from stress-strain relations, while out-of-plane counterparts σ_{xz}, σ_{yz}, σ_{zz} are calculated integrating local equilibrium equations (11).

III. NEW ADAPTIVE THEORIES OF THIS PAPER

New physically-based zig-zag theories of this paper are characterized by having an arbitrary displacement field freely chosen by the user, whose coefficients are redefined across the thickness so to satisfy constraints (9, 11-13). Such theories are generated without increasing the order of expansion with respect to the thickness coordinate and without to explicitly include zig-zag terms.

The possible choices of representation across the thickness of variables could be conjugated in infinite ways always different, the fantasy being the only limit. But whenever (9, 11-13) are simultaneously satisfied, accuracy and calculation times remain the same. Indeed, the analytical solution obtained via symbolic calculus always converges to the same result, which so assumes an asymptotic meaning with respect to the choice of representation.

The new adaptive theories are derived from the following generalized displacement field expressed as an infinite series of products of initially unknown amplitudes and exponential functions or any other basis of functions, comprising trigonometric and polynomial functions of the thickness coordinate [33]:

$$u_\alpha(x,y,z)=\left[\sum_{k=1}^{\infty} C^i_{k_\alpha}(x,y)e^{(k\,z_i/h_i)}\right]_{\Im}+\sum_{j=1}^{\Im} D^i_{j_\alpha}(x,y)$$

$$u_\varsigma(x,y,z)=\left[\sum_{k=1}^{\infty} C^i_{k_\varsigma}(x,y)e^{(k\,z_i/h_i)}\right]_{\Im}+\sum_{j=1}^{\Im} D^i_{j_\varsigma}(x,y) \qquad (19)$$

Coefficients are recalculated for each computational layer $\Im$ via symbolic calculus by enforcing the fulfillment of constraints (9,11-13). In particular the number of equilibria in different points of the thickness can be chosen in such a way as to determine the expressions of all the available coefficients remaining after the satisfaction of the boundary conditions. Theory (19) is here referred as ZZA-XX, but a further variant, called ZZA-XX' is also considered in the numerical applications for demonstration purposes, which is obtained assuming power series instead of exponential functions [33]:

$$u_\alpha(x,y,z)=\left[\sum_{k=1}^{\infty} C^i_{k_\alpha}(x,y)z^{(k)}\right]_{\Im}+\sum_{j=1}^{\Im} D^i_{j_\alpha}(x,y)$$

$$u_\varsigma(x,y,z)=\left[\sum_{k=1}^{\infty} C^i_{k_\varsigma}(x,y)z^{(k)}\right]_{\Im}+\sum_{j=1}^{\Im} D^i_{j_\varsigma}(x,y) \qquad (20)$$

The following theories are considered in the numerical illustrations, which are obtained as particular cases from (19) and (20). Different form of representation are chosen randomly to demonstrate what claimed about the possibility of arbitrarily choosing the representation without accuracy and cost change, if (9, 11-13) are simultaneously satisfied. They are developed starting from the general displacement field:

$$u_\alpha(x,y,z)=[\ u_\alpha{}^0(x,y)+z(\Gamma^0_\alpha(x,y)-w^0(x,y)_{,\alpha})\ ]_0+$$
$$+[\ \sum_{k=1}^{3} C^i_{k_\alpha}(x,y)\,{}^iF^k_\alpha(z)+C^i_\alpha\ ]_{i+c} \qquad (21)$$
$$u_\varsigma(x,y,z)=[\ w^0(x,y)\ ]_0+[\ \sum_{k=1}^{4} D^i_k(x,y)\,{}^iG^k(z)+C^i_\varsigma\ ]_{i+c}$$

Then particularizing the involved functions as follows

Even layers (i=2,4,…)

$$u_\alpha \rhd {}^iF^k_\alpha=\left\{\begin{matrix} z^{(k+1)/2} if\ k=1,3 \\ e^{(kz/(2h))}\ if\ k=2\end{matrix}(k_{\max}=3)\right\}$$
$$u_\beta \rhd {}^iF^k_\beta=\left\{z^k\quad (k=1,2,3)\right\}$$
$$u_\varsigma \rhd {}^iG^k=\left\{\begin{matrix} z^{(k+1)/2} if\ k=1,3 \\ e^{(kz/(2h))}\ if\ k=2,4\end{matrix}(k_{\max}=4)\right\}$$

ZZA_X_1 (22)

Odd layers (i=1,3,…)

$$u_\alpha \rhd {}^iF^k_\alpha=\left\{z^k\quad (k=1,2,3)\right\}$$
$$u_\beta \rhd {}^iF^k_\beta=\left\{\begin{matrix} z^{(k+1)/2} if\ k=1,3 \\ e^{(kz/(2h))}\ if\ k=2\end{matrix}(k_{\max}=3)\right\}$$
$$u_\varsigma \rhd {}^iG^k=\left\{z^k\quad (k=1,2,3,4)\right\}$$

Even layers (i=2,4,…)

$$u_\alpha \rhd {}^iF^k_\alpha=\left\{z^k\quad (k=1,2,3)\right\}$$
$$u_\beta \rhd {}^iF^k_\beta=\left\{\begin{matrix} z^{(k+1)/2} if\ k=1,3 \\ e^{(kz/(2h))}\ if\ k=2\end{matrix}(k_{\max}=3)\right\}$$
$$u_\varsigma \rhd {}^iG^k=\left\{\begin{matrix} z^{(k+1)/2} if\ k=1,3 \\ e^{(kz/(2h))}\ if\ k=2,4\end{matrix}(k_{\max}=4)\right\}$$

ZZA_X_2 (23)

Odd layers (i=1,3,…)

$$u_\alpha \rhd {}^iF^k_\alpha=\left\{\begin{matrix} z^{(k+1)/2} if\ k=1,3 \\ e^{(kz/(2h))}\ if\ k=2\end{matrix}(k_{\max}=3)\right\}$$
$$u_\beta \rhd {}^iF^k_\beta=\left\{\begin{matrix} z^{(k+1)/2} if\ k=1,3 \\ e^{(kz/(2h))}\ if\ k=2\end{matrix}(k_{\max}=3)\right\}$$
$$u_\varsigma \rhd {}^iG^k=\left\{z^k\quad (k=1,2,3,4)\right\}$$

ZZA_X_3 (24)

All layers (i=1,2,3,4…)

$$u_\alpha \rhd {}^iF^k_\alpha=\left\{\begin{matrix} z^{(k+1)/2} if\ k=1,3 \\ e^{(kz/(2h))}\ if\ k=2\end{matrix}(k_{\max}=3)\right\}$$
$$u_\beta \rhd {}^iF^k_\beta=\left\{\begin{matrix} z^{(k+1)/2} if\ k=1,3 \\ e^{(kz/(2h))}\ if\ k=2\end{matrix}(k_{\max}=3)\right\}$$
$$u_\varsigma \rhd {}^iG^k=\left\{\begin{matrix} z^{(k+1)/2} if\ k=1,3 \\ e^{(kz/(2h))}\ if\ k=2,4\end{matrix}(k_{\max}=4)\right\}$$

Even layers

$$u_\alpha \rhd {}^iF_\alpha^k = \left\{ z^k \quad (k=1,2,3) \right\}$$

$$u_\beta \rhd {}^iF_\beta^k = \left\{ \begin{matrix} z/h \\ \sin(z/h) \ \ if \ \ k=2 \\ e^{(kz/(2h))} \ \ if \ \ k=3 \end{matrix} (k_{\max}=3) \right\}$$

(i=2,4,…)

$$u_\varsigma \rhd {}^iG^k = \left\{ \begin{matrix} z^k if \ \ k=1,3 \\ e^{(z/h)} \ \ if \ \ k=2,4 \end{matrix} (k_{\max}=4) \right\}$$

ZZA_X_4 (25)

Odd layers

$$u_\alpha \rhd {}^iF_\alpha^k = \left\{ \begin{matrix} z^k if \ \ k=1,3 \\ e^{(z/h)} \ \ if \ \ k=2 \end{matrix} (k_{\max}=3) \right\}$$

$$u_\beta \rhd {}^iF_\beta^k = \left\{ \begin{matrix} z/h \\ \sin(z/h) \ \ if \ \ k=2 \\ e^{(kz/(2h))} \ \ if \ \ k=3 \end{matrix} (k_{\max}=3) \right\}$$

(i=1,3,…)

$$u_\varsigma \rhd {}^iG^k = \left\{ z^k \quad (k=1,2,3,4) \right\}$$

3.1 ZZA_RDFX and HWZZ_RDFX

The following additional theories are considered in numerical applications, in order to verify if theories with a lower order of expansion can be adequate and if the redefinition of the coefficients is the crucial aspect that improves considerably their accuracy with respect to counterparties with fixed coefficients.

ZZA_RDFX is a modified version of ZZA aimed at demonstrating that a different role can be attributed to coefficients than for ZZA, without any loss of accuracy:

$$\begin{aligned} u_\alpha(x,y,z) = & \left[\ u^0(x,y) + z(\Gamma_\alpha^0(x,y) - w^0(x,y)_{,\alpha}) \ \right]_0 + \\ & + \left[\ C_\alpha^i(x,y)z^2 + D_\alpha^i(x,y)z^3 \ \right]_i + \\ & + \left[\ \sum_{k=1}^{n_i} \Phi_\alpha^k(x,y)(z-z_k)H_k(z) + \sum_{k=1}^{n_3} {}_\alpha C_u^k(x,y)H_k(z) \ \right]_c \\ u_\varsigma(x,y,z) = & \left[\ w^0(x,y) \ \right]_0 + \left[\ b^i(x,y)z + c^i(x,y)z^2 + d^i(x,y)z^3 + \right. \\ & \left. + e^i(x,y)z^4 \ \right]_i + \left[\ \sum_{k=1}^{n_i} \Psi^k(x,y)(z-z_k)H_k(z) \right. \\ & \left. + \sum_{k=1}^{n_i} \Omega^k(x,y)(z-z_k)^2 H_k(z) + \sum_{k=1}^{n_3} C_\varsigma^k(x,y)H_k(z) \ \right]_c \end{aligned}$$

(26)

Differently to ZZA, terms Ω^k, Ψ^k, Φ_α^k, are calculated by imposing the fulfillment of (12) (for layers i>1), while C_α^i, d^i and e^i by enforcing (11) (for intermediate layers 1<i<nl). For the above layer (i=nl) Ω^k, Ψ^k, Φ_α^k allow the fulfillment of stress boundary conditions, while the remaining coefficients enable the fulfillment of stress continuity and enforcing local equilibrium equations.

It could be noticed that for some laminations in which one interface matches the middle reference plane, some stresses could be erroneously predicted to vanish for z=0; in order to ensure that each term could impose compatibility stress conditions (12) a different reference plane is assumed for this theory, whose origin has a distance that is $h_d > h/2$, while d.o.f. are still referred to middle reference plane:

$$\begin{aligned} u_\alpha(x,y,z) = & \left[\ u^0(x,y) + (z - h_d + h/2)(\Gamma_\alpha^0(x,y) + \right. \\ & \left. - w^0(x,y)_{,\alpha}) \ \right]_0 + \left[\ C_\alpha^i(x,y)z^2 + D_\alpha^i(x,y)z^3 \ \right]_i + \\ & \left[\ \sum_{k=1}^{n_i} \Phi_\alpha^k(x,y)(z-z_k)H_k(z) + \sum_{k=1}^{n_3} {}_\alpha C_u^k(x,y)H_k(z) \ \right]_c \\ u_\varsigma(x,y,z) = & \left[\ w^0(x,y) \ \right]_0 + \left[\ b^i(x,y)z + c^i(x,y)z^2 + \right. \\ & \left. + d^i(x,y)z^3 + e^i(x,y)z^4 \ \right]_i + \left[\ \sum_{k=1}^{n_i} \Psi^k(x,y)(z-z_k)H_k(z) + \right. \\ & \left. + \sum_{k=1}^{n_i} \Omega^k(x,y)(z-z_k)^2 H_k(z) + \sum_{k=1}^{n_3} C_\varsigma^k(x,y)H_k(z) \ \right]_c \\ & (h_d \le z \le h_d + h) \end{aligned}$$

(27)

HWZZ_RDFX assumes the same master displacement, strain and stress fields as HWZZ, but d^i terms (for i>1) enable the fulfillment of continuity of $\sigma_{\varsigma\varsigma,\varsigma}$ at each interface (the same reference plane of (26) is assumed). For this reason, HWZZ_RDFX has a lower computational burden than ZZA and HWZZ.

3.2 ZZA*_43X

A modified version of ZZA* whose in-plane displacements is a fourth-order piecewise polynomial, while the transverse one is piecewise cubic is assumed as:

$$\begin{aligned} u_\alpha(x,y,z) = & \left[\ u^0(x,y) + z(\Gamma_\alpha^0(x,y) - w^0(x,y)_{,\alpha}) \ \right]_0 + \left\{ \ \sum_{k=1}^{n_3} {}_k\tilde{B}_\alpha^i(x,y)z \ + \right. \\ & \left. + [C_\alpha^i(x,y)z^2] + [D_\alpha^i(x,y)z^3 + E_\alpha^i(x,y)z^4] + \sum_{k=1}^{n_i} {}_k\tilde{C}_\alpha^i(x,y) \ \right\}_{i+c} \\ u_\varsigma(x,y,z) = & \left[\ w^0(x,y) \ \right]_0 + \left\{ \ [b^i(x,y)z + \sum_{k=1}^{n_3} {}_k\tilde{b}^i(x,y)z] + \right. \\ & + [c^i(x,y)z^2 + \sum_{k=1}^{n_i} {}_k\tilde{c}^i(x,y)z^2] + \\ & \left. + [d^i(x,y)z^3] + \sum_{k=1}^{n_i} {}_k\tilde{d}^i(x,y) \ \right\}_{i+c} \end{aligned}$$

(28)

Similarly to ZZA*, terms are calculated by enforcing (9, 11-13), but similarly to ZZA_RDFX their role is exchanged, so, C_α^i, c^i and b^i impose the continuity of out-of-plane stresses for layers with i>1, while $\tilde{B}_\alpha^i$, ${}_k\tilde{b}^i$, ${}_k\tilde{c}^i$ enable the fulfillment of local equilibrium equations across the thickness for layers with i>1. For this theory the position of equilibrium points is more important than the parent theory and they should be chosen near layer interfaces, instead of within them. Anyway, results obtained demonstrate that also the expansion order of displacements can be reversed without any loss of

accuracy, if all physical constraints are enforced and coefficients redefined across the thickness.

3.3 HSDT_34X theory

This theory is a modified versions of HSDT whose coefficients are redefined across the thickness for each layer. In-plane displacements are piecewise cubic polynomial, while transverse one contain a sum of exponential, sinusoidal and power series functions. Its displacement field is:

$$u_\alpha(x,y,z) = [\ u^0(x,y) + z(\Gamma^0_\alpha(x,y) - w^0(x,y)_{,\alpha})\ ]_0 + B^i_\alpha(x,y)z + \\ + C^i_\alpha(x,y)z^2 + D^i_\alpha(x,y)z^3$$

$$u_\varsigma(x,y,z) = [\ w^0(x,y)\ ]_0 + b^i(x,y)z + c^i(x,y)\exp(z/h) + \\ + d^i(x,y)\sin(\pi z/2h) + e^i(x,y)\cos(\pi z/2h) \qquad (29)$$

Results will show that HSDT_34X, whose coefficients are obtained by imposing the full set of physical constraints (9, 11-13) provide indistinguishable results from other higher-order theories. This demonstrate that all theories that are capable to at least describe piecewise cubic in-plane and piecewise fourth order polynomial transverse displacements, are able to get precise results with quite affordable time calculations.

IV. NUMERICAL ILLUSTRATIONS

A number of elasto-static challenging benchmarks having pronounced layerwise effects is considered in order to assess the accuracy of theories. Such benchmarks are chosen being of practical interest and because in addition to an adequate description of transverse shear effects, as many others in literature, they also require a very accurate modeling of the transverse normal deformation. This latter effect is important as it manifests for lay-ups, loading and boundary conditions that find industrial applications, like ones here examined, consequently it cannot be neglected and thus represents a challenge for researchers because they are called to develop theories efficiently capturing it.

The numerical assessments presented aim to confirm, extend and generalize previous findings by the authors [16], [17]. Besides showing the capability of the theories considered to accurately describe transverse shear and normal deformations effects with a small number of d.o.f. they aim to highlight that whenever the full set of physical constraints (9, 11-13) is enforced. This gives the present theories the appellation of physically-based. The representation of variables across the thickness and zigzag functions can be completely arbitrarily chosen without the results changing. In detail, results aim to show that once (9, 11-13) are enforced simultaneously, as for the refined physically-based zig-zag theories of this paper, (i) zig-zag functions and the functions used to represent variables across the thickness can be arbitrarily chosen without any change in the degree of accuracy, while getting a cost benefit. Moreover, (ii) zig-zag functions can even be omitted, so getting further benefits, provided that a sufficient number of coefficients is still incorporated in the displacement field, whose expressions are redefined across the thickness through the enforcement of (9, 11-13). In consequence of all this, (iii) a different representation can be chosen for each displacement, which also can vary from point-to-point across the thickness. Likewise, different zig-zag functions can be chosen for each single displacement (variable-kinematics form) without any accuracy loss. Furthermore, (iv) a specific role need not be assigned to individual coefficients of displacements, as they can be freely re-defined once their expressions are re-defined across the thickness. Because lower-order theories which reduce calculation costs being already accurate are of great interests to designers examples of these theories are considered. It is shown that, confirming results in the literature, they can be accurate for certain cases but not in general. Moreover, (v) a partial fulfilment of (9, 11-13) implies the loss of validity of (i) to (iv), as shown by other theories in the literature.

Case a

Firstly. a simply supported laminated beam [0/-90/0/-90] under sinusoidal load, retaken from [17], is analysed, that is used as a reference test for theories. Nevertheless all layers are made of same material, because its antisymmetric lay-up, there are quite strong 3-D effects. This case is interesting, because it shows that a periodical stack-up does not necessarily involve a slope sign reversal at interfaces of displacements, so, Murakami's rule is not satisfied. Indeed, MHR and MHR4 theories, two HR mixed theories that include Murakami's zig-zag functions and whose coefficients are not redefined layer-by-layer across the thickness (see [17]) cannot provide the right trend of in-plane displacement at first interface from above (see Figure 1 and Table 5) and also the transverse displacement is not adequately described. Better results of displacements are obtained by MHWZZA and MHWZZA4, two HW mixed theories whose displacements are the same of MHR, while strains and stresses are assumed apart and coincident with those of HWZZ (MHWZZA4 include also transverse displacement of ZZA) and also by MHR± and MHR4±. These theories are retaken from [17] and assume the same displacements of MHR and MHR4 respectively, but unlike them the sign of Murakami's zig-zag function is calculated on a physical basis, instead of being forced to reverse at each interface, comparing the lowest norm of the residual force coming from the

three local equilibrium equations. Moreover, HRZZ and HRZZ4, two physically-based HR theory with a uniform and a polynomial transverse displacement, respectively, cannot obtain the right trend of u_ς. Despite this, all theories of Figure 1 are able to obtain the accurate stresses across the thickness, making this case not particularly probative. All theories discussed in this paper provide always results that are in very good agreement with exact and 3-D FEA ones. So, it is demonstrated that only higher-order adaptive physically-based theories, namely whose coefficients are redefined across the thickness imposing all the physical constraints (9, 11-13), can assume different zig-zag functions, omit them or change the representation without any loss of accuracy. All theories of this paper from section 2.2 to section 3.3 are very accurate and have a computational burden similar to each other and to FSDT. Those without zig-zag functions, namely ZZA* and theories of section 3, are the most efficient as shown in Table 4. The other theories previously developed by authors and not discussed here but reported in numerical results, can have lower processing times lower but are inaccurate.

Case b

This case pertains a simply-supported, rectangular sandwich plate with a length-to thickness ratio $l_x / h = 4$ and a side ratio $l_y / l_x = 3$, having a stiffer core and a damaged, weaker lower face [17] (see Table 2b). Results are reported in Figure 2 and Table 6. Currently the slope of u_α and u_β is reversing at the interfaces, as prescribed by Murakami's zig-zag function, nevertheless the through-thickness variation of in-plane components is incorrectly predicted by theories MHR, MHR4, MHWZZA and MHWZZA4 using it, specially across the core. As the others lower-order theories are also inaccurate, it turns out that also in this case layerwise effects assume a paramount importance because geometric and material asymmetries act jointly in strengthening them, so that the non-compliance with stress-compatibility conditions (12), or a only a partial respect of the remaining constraints (9), (11), (13) leads to a considerable loss of accuracy.

From the examination of results it may be concluded that theories using Di Sciuva's like zig-zag functions provides a much better representation of slope changes at interfaces than theories using Murakami's zig-zag functions. In general, it can be stated that all theories allowing a redefinition of coefficients through the redefinition of zig-zag amplitudes at layer interfaces as well as those which do not explicitly contain zig-zag functions but implement this definition through the satisfaction of (9, 11-13) are much accurate. It can be observed that transverse shear stresses are quite accurately reproduced by all theories except by MHR at the lower face, so in the present case an incorrect representation of u_ς doesn't have effects, as it is reputed that the lower elastic moduli of the damaged face prevent the spreading of errors across the thickness. Adaptive theories of this paper are very efficient (see Table 4) but the best ones, from this standpoint are ZZA* and theories of section 3 without zig-zag functions.

Case c

This case pertains a three-layer, simply-supported sandwich plate under sinusoidal loading. Currently, a damaged and thinner lower face and a thicker core (that is partially damaged up to 0.15h from below, see Table 2b) are considered in order to extol the layerwise effects played by the transverse displacement within a range of material and geometric properties of practical interest.

Figure 3 and Table 7 report through-thickness displacement and stress fields for this case. Of particular interests are $\sigma_{\alpha\varsigma}$ across the thickness at $x = 0$, $y = Ly/2$ and $\sigma_{\beta\varsigma}$ at $x = Lx/2$, $y = 0$. Results of 3-D FEA for this case show that none of the three elastic displacement components exhibits a slope change at the interfaces of core, so Murakami's zig-zag function requirement isn't satisfied. Because of this, MHR and MHR4 incorrectly predict the through-thickness variation of in-plane displacements u_α and u_β as well as the transverse displacement u_ς (the largest discrepancies are shown as regards this displacement), while HRZZ4, MHR and MHR4 underestimate it.

Now capturing stress field becomes challenging because transverse shear stresses are strongly asymmetric across the thickness and the sign of $\sigma_{\beta\varsigma}$ is reversing near the lower face. Moreover, also the transverse normal stress exhibits a through-thickness sign change. Currently, the deficiency of lower-order theories (that accurately predict in-plane stresses) stands out as an incorrect prediction of $\sigma_{\varsigma\varsigma}$ across the core. It represents a crucial matter because it implies defects of lower-order mixed theories that couldn't be recovered in the post-process phase. As a consequence of errors made in the representation of u_ς, these theories predict an incorrect $\sigma_{\alpha\varsigma}$ across the lower face and core. Lower errors are made for $\sigma_{\beta\varsigma}$, with the exception of MHR and MHR4 that provide an

incorrect prediction anywhere across the thickness. Once again the processing time of Table 4 shows that the most efficient theories are adaptive theories without zig-zag functions.

Case d

Figure 4 and Table 8 report $u_\alpha, \sigma_{\alpha\xi}$ at $x = 0$ and u_ς, $\sigma_{\alpha\alpha}$ and $\sigma_{\varsigma\varsigma}$ at $x = L_x / 4$ where the strongest variations of the reference solutions occur for this case assuming a step loading,

The results highlight that step loading enhances layerwise effects so much that lower order theories cannot achieve the same accuracy of adaptive theories of this paper, that however don't require higher computational burden.

Irrespective the two positions considered, MHR and MHR4 inaccurately predict the in-plane displacement u_α everywhere across the thickness, while HRZZ, HRZZ4, MHWZZA and MHWZZA4 that benefit of displacement and/or stress fields of ZZA and HWZZ provide predictions in a well agreement each other and with FEA 3-D. Currently HRZZ, MHWZZA and MHWZZA4 incorrectly predict the transverse displacement u_ς across the thickness, while lower errors are shown for the bending stress $\sigma_{\alpha\alpha}$, except MHR, MHR4 that are a little inaccurate across the lower face. Instead, all lower order theories incorrectly predict the transverse shear stress $\sigma_{\alpha\varsigma}$ and the transverse normal stress $\sigma_{\varsigma\varsigma}$. Nevertheless all adaptive theories are very efficient, also in this case those without zig-zag coefficients are the most performing (see Table 4). Moreover, their results are indistinguishable, irrespective of the choice of zig-zag or representation functions.

Case e

This case pertains the same eleven-layers sandwich beam of [27] but currently a step loading is assumed. Figure 9 and Table 9 report the through-thickness distribution of $\sigma_{\alpha\xi}$ at $x = 0$, u_α at $x = L_x / 2$, u_ς, $\sigma_{\alpha\alpha}$ and $\sigma_{\varsigma\varsigma}$, i.e. at positions where discrepancies among theories are most striking. It can be observed that the through-thickness distribution of transverse shear stress is quite different from that of [16], as well as that larger discrepancies of results are observed, with the exception of $\sigma_{\alpha\alpha}$ that is well described by all theories considered in this paper.

Regardless the two position considered, the slope of in-plane and transverse displacements doesn't reverse at each interface, so, Murakami's zig-zag function isn't suitable. As a consequence, once again MHR and MHR4 are inaccurate and, in particular, they incorrectly predict u_α nearby the core upper interface. The assumption of stress, strain and transverse displacement apart improves the accuracy of mixed theories MHWZZA and MHWZZA4, but again the variation of the in-plane displacement is misestimated, so these theories can obtain only a partial recovery of errors, so it can be concluded that post-processing techniques improves accuracy of stresses but have only a marginal effect on displacements, as was to be expected.

HRZZ and HRZZ4 calculate quite accurately the in-plane displacement at each position, therefore it results again the superior accuracy of Di Sciuva's like zig-zag function over Murakami's one. A grater dispersion of results is shown for the transverse displacement since only the piecewise representation of u_ς by adaptive theories of this paper are adequate.

Errors to a lesser extent are made as regards stresses $\sigma_{\alpha\alpha}$ and $\sigma_{\alpha\varsigma}$ by all lower-order theories with the exception of MHR and MHR4, as these latter theories give incorrect predictions everywhere across the core. Anyway, only adaptive theories of this paper appear always and everywhere very accurate and low cost (see Table 4).

Case f

This case is a propped-cantilever sandwich beam under a uniform loading. At x=Lx only lower edge is supported. A length-to-thickness ratio of 20 is assumed. Nevertheless this case is not extremely thick, there are discrepancies among the predictions of theories (see Figure 6 and Table 10), because layerwise effects are strong and only adaptive theories of this paper provide results in a well agreement with those obtained by 3-D FEA, while not costing more than the other ones. Transverse shear stress is wrongly predicted by HRZZ, HRZZ4, MHR, MHR4, MHR±, MHR4±, MHWZZA and MHWZZA4 and also transverse normal one is incorrectly obtained by these latter theories.

It should be noticed that the slope of in-plane displacement reverses at each interface, as postulated by Murakami's rule, but results provided by MHR, MHR4, MHR± and MHR4± are wrong, also for transverse displacement, because their kinematics is too poor. Displacements are also incorrectly predicted by MHWZZA, MHWZZA4, HRZZ4 and HRZZ (the latter theory gives the worst trend of transverse displacement).

V. CONCLUSION

A number of new zig-zag theories with a different representation of variables across the

thickness and differently assuming zig-zag functions, so ultimately differently accounting for layerwise effects, have been developed an compared with previously developed zig-zag theories by the authors in displacement-based and mixed form, some having features similar to those of theories already proposed in the literature. All the theories considered have the same five functional degrees of freedom like FSDT and HSDT so their number of unknowns is independent from the number of constituent layers and the memory storage occupation is minimal.

Challenging elastostatic benchmarks have been considered to show on a rather broad way with respect to previous papers by the authors [16], [17] that whenever the expressions of coefficients of displacements are determined a priori by enforcing the fulfillment of the full set of interfacial stress compatibility conditions, of stress boundary conditions and of local equilibrium equations at a number of selected point sufficient to determine the expressions of all coefficients, the choice of the representation form and of zig-zag functions can be arbitrary without the results changing. To compare theories under the same conditions, the same trial functions and expansion order are used to obtain closed form solutions. Distributed or localized loading and simply-supported and clamped edges have been considered along with with distinctly different material properties and thickness of layers. Higher-order zig-zag theories, whose coefficients are redefined layer-by-layer by imposing the fulfillment of interfacial displacement and stress compatibility conditions, stresses boundary conditions at upper and lower bounding faces and local equilibrium equations at different points across the thickness proved to be always those most accurate and efficient, their computational burden being still comparable to that of equivalent single-layer theories with th same number of d.o.f. Under these conditions it is proven by numerical results that zig-zag functions can even be omitted, with a considerable advantage from the standpoint of computational costs. Zig-zag functions can be arbitrarily chosen and variables can be assumed in an arbitrary form, i.e. different form one to another and from region to region across the thickness, without the results changing. Moreover, it is shown that assigning a specific role to individual coefficients of displacements is immaterial, as the role can be freely varied provided that the same total number of coefficients is maintained and expressions are determined by enforcing all physical constraints above mentioned. The expansion order of displacements can be freely chosen but a great accuracy is already obtained with a cubic/quartic assumption of in-plane and transverse displacements, or vice versa.

Theories ZZA, ZZA*, HWZZ, HWZZM, HWZZM*, ZZA-XX, ZZA-XX', ZZA_X_1 to ZZA_X_4, ZZA_RDFX, HWZZ_RDFX, ZZA*_43X, HSDT_34X with totally different forms of representation prove to be equally accurate and efficient. However the most efficient theories are shown to be ZZA*, HWZZM*, ZZA-XX, ZZA-XX', ZZA_X_1 to ZZA_X_4, ZZA_RDFX, HWZZ_RDFX, ZZA*_43X, HSDT_34X wherein the explicit presence of zig-zag functions is omitted. So all this mentioned theories can be used to carry out 3-D analyses more conveniently3-D finite element methods and discrete-layer models in the cases where domain is quite simple. Lower-order theories HRZZ, HRZZ4, MHWZZA, MHWZZA4, in particular ones that incorporate Murakami's zig-zag function MHR and MHR4 cannot be employed for the same purpose being inaccurate, even if not always. The general rule that can be drawn is that the higher-order zigzag theories of this paper with a redefinition of the coefficients are always accurate and efficient and therefore usable for any case.

REFERENCES

[1]. E. Carrera, A study of transverse normal stress effects on vibration of multilayered plates and shells, Journal of Sound and Vibration, 225, 1999, 803–829.

[2]. E. Carrera, A. Ciuffreda, Bending of composites and sandwich plates subjected to localized lateral loadings: a comparison of various theories, Composite Structures, 68, 2005, 185–202.

[3]. E. Carrera, Developments, ideas, and evaluations based upon Reissner's mixed variational theorem in the modeling of multilayered plates and shells, Appl. Mech. Rev. 54, 2001, 301-329.

[4]. E. Carrera, Historical review of zig-zag theories for multilayered plates and shells. Appl. Mech. Rev, 56, 2003 1-22.

[5]. E. Carrera, On the use of the Murakami's zig-zag function in the modeling of layered plates and shells, Compos. Struct, 82, 2004, 541–554.

[6]. L. Demasi, Refined multilayered plate elements based on Murakami zig-zag functions, Compos. Struct., 70, 2004, 308–316.

[7]. V.V. Vasilive, S.A. Lur'e, On refined theories of beams, plates and shells. J. Compos. Mat., 26, 1992 422–430.

[8]. J.N. Reddy, D.H. Robbins, Theories and computational models for composite laminates. Appl. Mech. Rev., 47, 1994, 147–165.

[9]. S.A. Lur'e, N. P. Shumova, Kinematic models of refined theories concerning composite beams plates and shells, Int. J. Appl. Mech., 32, 1996, 422-430.
[10]. A.K. Noor, S.W. Burton, C.W. Bert, Computational model for sandwich panels and shells, Appl. Mech. Rev, 49, 1996, 155–199.
[11]. H. Altenbach, Theories for laminated and sandwich plates. A review. Int. J. Appl. Mech. 34, 1998, 243-252.
[12]. R. Khandan, S. Noroozi, P. Sewell, J. Vinney, The development of laminated composite plate theories: a review, J. Mater. Sci. 47, 2012, 5901-5910.
[13]. S. Kapuria, J.K. Nath, On the accuracy of recent global–local theories for bending and vibration of laminated plates. Compos. Struct. 95, 2013, 163–172.
[14]. J.N. Reddy, Mechanics of laminated composite plates and shells: Theory and analysis, 2nd ed. (CRC Press: Boca Raton, United States, 2003).
[15]. U. Icardi, F. Sola, Development of an efficient zig-zag model with variable representation of displacements across the thickness. J. of Eng. Mech, 140, 2014, 531-541.
[16]. U. Icardi, A. Urraci, Free and forced vibration of laminated and sandwich plates by zig-zag theories differently accounting for transverse shear and normal deformability. Aerosp. MDPI., 5, 2018 108.
[17]. U. Icardi, A. Urraci, A. Novel HW mixed zig-zag theory accounting for transverse normal deformability and lower-order counterparts assessed by old and new elastostatic benchmarks. Aer. Sci. & Tech., 80, 2018 541-571.
[18]. K.N. Cho, C.W. Bert, A.G. Striz. Free vibrations of laminated rectangular analyzed by higher order individual-layer theory. Journal of Sound and Vibration 145(3), 1991, 429-442.
[19]. A. K. Barouni, D.A. Saravanos. A layerwise semi-analytical method for modeling guided wave propagation in laminated and sandwich composite strips with induced surface excitation. Aerospace Science and Technology, 51, 2016, 118–141.
[20]. Y. Frostig, O.T. Thomsen. High-order free vibration of sandwich panels with a flexible core, International Journal of Solids and Structures, 41, 2004, 1697–1724..
[21]. M.K. Rao, Y.M. Desai. Analytical solutions for vibrations of laminated and sandwich plates using mixed theory. Composite Structures, 63, 2004, 361–373.
[22]. W. Zhen, C. Wanji, Free vibration of laminated composite and sandwich plates using global–local higher-order theory, Journal of Sound and Vibration 298, 2006 333–349.
[23]. S. Kapuria, P.C. Dumir, N.K. Jain, Assessment of zig-zag theory for static loading, buckling, free and forced response of composite and sandwich beams, Composite Structures, 64, 2004, 317–327.
[24]. V.N. Burlayenko, H. Altenbach, T. Sadowski. An evaluation of displacement-based finite element models used for free vibration analysis of homogeneous and composite plates, Journal of Sound and Vibration, 358, 2015, 152–175.
[25]. L. Jun, H. Xiang, L. Li Xiaobin, Free vibration analyses of axially loaded laminated composite beams using a unified higher-order shear deformation theory and dynamic stiffness method, Composite Structures, 158, 2016, 308–322.
[26]. M. Di Sciuva, A refinement of the transverse shear deformation theory for multilayered orthotropic plates. L'Aerot. Miss. & Spaz., 62, 1984, 84–92.
[27]. U. Icardi, Higher-order zig-zag model for analysis of thick composite beams with inclusion of transverse normal stress and sublaminates approximations. Compos. Part B. 32, 2001, 343-354.
[28]. S. Brischetto, E. Carrera, L. Demasi, Improved response of asymmetrically laminated sandwich plates by using Zig-Zag functions. J. Sandwich Struct. & Mat, 11, 2009, 257- 267.
[29]. A. Catapano, G. Giunta, S. Belouettar, E. Carrera, Static analysis of laminated beams via a unified formulation. Compos. Struct. 94, 2011, 75-83.
[30]. A.G. de Miguel, E. Carrera, A. Pagani, E. Zappino, Accurate Evaluation of Interlaminar Stresses in Composite Laminates via Mixed One-Dimensional Formulation, AIAA Journal, 56, 2018, 4582-4594.
[31]. W. Zhen, C. Wanji, A study of global–local higher-order theories for laminated composite plates. Compos. Struct., 79, 2007, 44–54.
[32]. Y. Yang, A. Pagani, E. Carrera. Exact solutions for free vibration analysis of laminated, box and sandwich beams by refined layer-wise theory. Composite Structures, 175, 2017, 28–45.
[33]. A. Urraci, Development of accurate and efficient structural models for analysis of

multilayered and sandwich structures of industrial interest, Still unpublished PhD thesis, Aerospace Engineering, Politecnico di Torino

Table 1: Acronyms; in bold the new teories; $^{(n)}$ degree of displacements

Acronym	Description(section)	Acronym	Description(section)
FEA-3D	Mixed solid finite elements [31].	MHWZZA	Mixed HW theory [17].
HRZZ	Mixed HR theory, $u^{(3)}_{\alpha,\beta}$, $u^{(0)}_{\varsigma}$, [17].	MHWZZA4	Mixed HW theory [17].
HRZZ4	Mixed HR theory, $u^{(3)}_{\alpha,\beta}$, $u^{(4)}_{\varsigma}$, [17]	ZZA	$u^{(3)}_{\alpha,\beta}$, $u^{(4)}_{\varsigma}$ zig-zag adaptive theory [15] (2.2).
HSDT_34X	Enriched adaptive versions of HSDT $u^{(3)}_{\alpha,\beta}$, $u^{(4)}_{\varsigma}$ (3.3).	ZZA*	$u^{(3)}_{\alpha,\beta}$, $u^{(4)}_{\varsigma}$ modified ZZA [16] (2.3).
HWZZ	HW mixed version of ZZA [17] (2.4).	ZZA*_43X	$u^{(4)}_{\alpha,\beta}$, $u^{(3)}_{\varsigma}$ modified version of ZZA* (3.2).
HWZZ_RDFX	Modified HWZZ theory (3.1).		
HWZZM	HWZZ with different zig-zag functions [16] (2.5).	ZZA_RDFX	Modified ZZA theory (3.1).
HWZZM*	HWZZ with different zig-zag functions [16] (2.6).	ZZA_X_1 ZZA_X_2 ZZA_X_3 ZZA_X_4	$u^{(3)}_{\alpha,\beta}$, $u^{(4)}_{\varsigma}$ modified ZZA theories, with different representation across the thickness (3).
MHR	Mixed HR theory $u^{(3)}_{\alpha,\beta}$ with Murakami's zig-zag function , $u^{(4)}_{\varsigma}$ lacking, [17]	ZZA-XX	Zig-zag general theory with exponential representation [33] (3).
MHR4	Mixed HR theory, displacements with Murakami's zig-zag function [17].	ZZA-XX'	Zig-zag general theory with power representation [33] (3).

Table 2a: Casuistry

Case	Lay-up	Layer thickness	Material		Loading	Lx/h	Ly/Lx
a (*§)	[0/-90/0/-90]	$[0.25h]_4$	$[p]_4$		$p^0(x) = p^0_u \sin(\pi x / L_x)$ if $0 \le x \le L_x$	4	-
b (§)	[0/0/0]	[0.2h/0.7h/0.1h]	[c2/c2/c2]	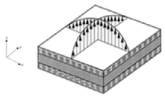	$p^0(x,y) = p^0_u \sin(\pi x / L_x)\sin(\pi y / L_y)$ if $0 \le x \le L_x$ and $0 \le y \le L_y$	4	3
c (*↓§)	[0/0/0]	[0.05h/0.85h/0.10h]	[p/mc/p]			4	1
d (*§)	$[90/0_5/90]$	$[0.1h_2/0.2h_3/0.1h_2]$	$[pf_2/pvc/hh]_s$		$p^0(x) = \begin{cases} p^0_u & \text{if } 0 \le x \le L_x/2 \\ -p^0_u & \text{if } L_x/2 \le x \le L_x \end{cases}$	8	-
e (*§)	$[0]_{11}$	[0.01h / 0.025h / 0.015h / 0.02h / 0.03h / 0.4h]$_s$	$[1/2/3/1/3/4]_s$			4	-
f (*§)	[0/0/0]	[(2h/7) / (4h/7) / (h/7)]	[n/n/n]		$p^0(x) = p^0_u$ if $0 \le x \le L_x$	20	-

Whether Murakami's function assumption is not satisfied by u_α (*), u_β (↓) and u_ς (§)

Table 2b: Trial Functions, expansion order, normalization and damage properties

Case	Trial functions	Expansion	Normalization	Damaged Layers	Damaged Coefficients	Damaged Properties
a	$u^0(x,y)=\sum_{m=1}^{M}A_m\cos\left(\frac{m\pi x}{L_x}\right);$ $w^0(x,y)=\sum_{m=1}^{M}C_m\sin\left(\frac{m\pi x}{L_x}\right);$ $\gamma_x^0(x,y)=\sum_{m=1}^{M}D_m\cos\left(\frac{m\pi x}{L_x}\right)$	1	$\bar{u}_\alpha=\frac{E_2u_\alpha(0,z)}{hp^0}$ $\bar{u}_\zeta=\frac{u_\zeta\left(\frac{L_y}{2},z\right)}{hp^0}$ $\bar{\sigma}_{\alpha\alpha}=\frac{\sigma_{\alpha\alpha}\left(\frac{L_x}{2},z\right)}{p^0}$ $\bar{\sigma}_{\alpha\zeta}=\frac{\sigma_{\alpha\zeta}(0,z)}{p^0}$ $\bar{\sigma}_{\zeta\zeta}=\frac{\sigma_{\zeta\zeta}\left(\frac{L_x}{2},z\right)}{p^0}$	-	-	-
b	$u^0(x,y)=\sum_{m=1}^{M}\sum_{n=1}^{N}A_{mn}\cos\left(\frac{m\pi}{L_x}x\right)\sin\left(\frac{n\pi}{L_y}y\right);$ $v^0(x,y)=\sum_{m=1}^{M}\sum_{n=1}^{N}B_{mn}\sin\left(\frac{m\pi}{L_x}x\right)\cos\left(\frac{n\pi}{L_y}y\right);$ $w^0(x,y)=\sum_{m=1}^{M}\sum_{n=1}^{N}C_{mn}\sin\left(\frac{m\pi}{L_x}x\right)\sin\left(\frac{n\pi}{L_y}y\right);$ $\gamma_x^0(x,y)=\sum_{m=1}^{M}\sum_{n=1}^{N}D_{mn}\cos\left(\frac{m\pi}{L_x}x\right)\sin\left(\frac{n\pi}{L_y}y\right);$ $\gamma_y^0(x,y)=\sum_{m=1}^{M}\sum_{n=1}^{N}E_{mn}\sin\left(\frac{m\pi}{L_x}x\right)\cos\left(\frac{n\pi}{L_y}y\right);$	1	$\bar{u}_\alpha=\frac{u_\alpha\left(0,\frac{L_y}{2},z\right)}{hp^0}$ $\bar{u}_\beta=\frac{u_\beta\left(\frac{L_x}{2},0,z\right)}{hp^0}$ $\bar{u}_\zeta=\frac{u_\zeta\left(\frac{L_x}{2},\frac{L_y}{2},z\right)}{hp^0}$ $\bar{\sigma}_{\alpha\alpha}=\frac{\sigma_{\alpha\alpha}\left(\frac{L_x}{2},\frac{L_y}{2},z\right)}{p^0(L_x/h)^2}$ $\bar{\sigma}_{\beta\beta}=\frac{\sigma_{\beta\beta}\left(\frac{L_x}{2},\frac{L_y}{2},z\right)}{p^0(L_x/h)^2}$ $\bar{\sigma}_{\alpha\beta}=\frac{\sigma_{\alpha\beta}(0,0,z)}{p^0(L_x/h)^2}$ $\bar{\sigma}_{\alpha\zeta}=\frac{\sigma_{\alpha\zeta}\left(0,\frac{L_y}{2},z\right)}{p^0}$ $\bar{\sigma}_{\beta\zeta}=\frac{\sigma_{\beta\zeta}\left(\frac{L_x}{2},0,z\right)}{p^0}$ $\bar{\sigma}_{\zeta\zeta}=\frac{\sigma_{\zeta\zeta}\left(\frac{L_x}{2},\frac{L_y}{2},z\right)}{p^0}$	Layer 1	$2\cdot10^{-1}$	E_{1111} E_{1122} E_{2222} E_{1212}
c		1		Layer 1 Layer 2*	$1\cdot10^{-2}$ $2\cdot10^{-1}$	E_{1111} E_{1122} E_{2222} E_{1212} E_{1122} E_{2222} E_{1212} E_{1313} E_{2323}
d	$u^0(x,y)=\sum_{m=1}^{M}A_m\cos\left(\frac{2m\pi x}{L_x}\right);$ $w^0(x,y)=\sum_{m=1}^{M}C_m\sin\left(\frac{2m\pi x}{L_x}\right);$ $\gamma_x^0(x,y)=\sum_{m=1}^{M}D_m\cos\left(\frac{2m\pi x}{L_x}\right)$	1	$\bar{u}=\frac{u\left(\frac{L_x}{2},z\right)}{hp^0}$ $\bar{w}=\frac{w\left(\frac{L_x}{4},z\right)}{hp^0}$ $\bar{\sigma}_{xx}=\frac{\sigma_{xx}\left(\frac{L_x}{4},z\right)}{p^0(L_x/h)^2}$ $\bar{\sigma}_{xz}=\frac{\sigma_{xz}(0,z)}{p^0}$ $\bar{\sigma}_{zz}=\frac{\sigma_{zz}\left(\frac{L_x}{4},z\right)}{p^0}$	-	-	-
e		1		-	-	-
f	$u^0(x,y)=\sum_{i=1}^{I}A_i\left(\frac{x}{L}\right)^i;$ $w^0(x,y)=\sum_{i=1}^{I}C_i\left(\frac{x}{L}\right)^i;$ $\gamma_x^0(x,y)=\sum_{i=1}^{I}D_i\left(\frac{x}{L}\right)^i$	9	$\bar{u}=\frac{u(L_x,z)}{hp^0}$ $\bar{w}=\frac{w(L_x,z)}{hp^0}$ $\bar{\sigma}_{xx}=\frac{\sigma_{xx}(L_x,z)}{p^0(L_x/h)^2}$ $\bar{\sigma}_{xz}=\frac{A\sigma_{xz}(L_x,z)}{P^0L_x}$ $\bar{\sigma}_{zz}=\frac{\sigma_{zz}(L_x,z)}{p^0}$			

*As regards this layer, only a part from below (thick 0.15h) is damaged

Table 3. Mechanical properties.

Material name	1	2	3	4	c2 [iso]	hh	mc	p	pf	pvc	n [iso]
E1[GPa]	1	33	25	0.05	-	250×10^{-3}	0.1	172.4	25×10^{3}	25×10^{1}	-
E2[GPa]	1	1	1	0.05	-	250×10^{-3}	0.1	6.89	1×10^{3}	25×10^{1}	-
E3 [GPa]	1	1	1	0.05	M1	2500×10^{-3}	0.1	6.89	1×10^{3}	25×10^{1}	M2
G12 [GPa]	0.2	0.8	0.5	0.0217	-	1×10^{-3}	0.04	3.45	5×10^{2}	9.62×10^{1}	-
G13 [GPa]	0.2	0.8	0.5	0.0217	-	875×10^{-3}	0.04	3.45	5×10^{2}	9.62×10^{1}	-
G23 [GPa]	0.2	0.8	0.5	0.0217	-	1750×10^{-3}	0.04	1.378	2×10^{2}	9.62×10^{1}	-
υ12	0.25	0.25	0.25	0.15	0.34	0.9	0.25	0.25	0.25	0.3	0.33
υ13	0.25	0.25	0.25	0.15	0.34	3×10^{-5}	0.25	0.25	0.25	0.3	0.33
υ23	0.25	0.25	0.25	0.15	0.34	3×10^{-5}	0.25	0.25	0.25	0.3	0.33

M1 $E_l/E_u=5/4$, $E_l/E_c=10^4$; M2 $E_u/E_l=1.6$, $E_u/E_c=166.6\cdot10^5$; [iso]=isotropic $E_1=E_2=E_3$ $G_1=G_2=G_3$

Table 4: Processing time [s] on a computer with quad-core CPU@2.60GHz, 64-bit OS and 8.00 GB RAM; errors: ♥ > 3%; ♣ > 10%.

		Theory	**Case**					
			a	**b**	**c**	**d**	**e**	**f**
	Reference theory	FSDT	2.7860	4.1470	5.0712	6.2168	6.5481	4,0522
General theories	(arbitrary representation)	ZZA_X_1	10.2237	7.9699	7.7923	14.8450	13.2839	12.0660
		ZZA_X_2	10.4743	8.1551	8.0180	15.2373	13.6303	12.4211
		ZZA_X_3	10.6675	8.3169	8.1517	15.4161	13.8690	12.5162
		ZZA_X_4	10.6481	8.2816	8.1362	15.4323	13.8039	12.6003
Mixed HR	(uniform w) (polynomial w4)	HRZZ	♥14.9182	♥11.5234♣	♥11.6618♣	♥20.2183♣	♥20.9194♣	♥18.2261♣
		HRZZ4	♥14.7821	♥11.8083♣	♥11.4963♣	♥20.6428♣	♥21.1942♣	♥18.4891♣
	(Murakami's zig zag u3,v3)	MHR	♥8.1514♣	♥6.7454♣	♥6.8583♣	♥11.4933♣	♥12.0285♣	♥6.6258♣
		MHR±	♥8.6016♣	♥6.7688♣	♥6.9558♣	♥12.5430♣	♥12.3437♣	♥6.7160♣
	(Murakami's zig zag u3,v3,w4)	MHR4	♥8.6564♣	♥6.5908♣	♥6.2430♣	♥11.4761♣	♥12.5987♣	♥6.9702♣
		MHR4±	♥9.2370♣	♥6.7213♣	♥6.3437♣	♥12.5583♣	♥12.8111♣	♥7.0373♣
Mixed HW	(no zig-zag functions)	HWZZ	12.0193	6.4675	6.5745	18.4597	15.1594	12.8490
		HWZZ_RDFX	11.8948	9.2171	9.0704	17.2278	15.5294	14.0459
		HWZZM*	10.0139	7.7776	7.6312	14.5394	12.9410	11.7302
	(Murakami's zig zag u^3,v^3,w^4)	HWZZM	10.9757	8.5366	8.3743	15.9133	14.2983	12.8841
		MHWZZA	♥10.7396♣	♥8.2660♣	♥8.3921♣	♥16.9729♣	♥14.1698♣	♥7.6952♣
		MHWZZA4	♥10.2451♣	♥8.5094♣	♥8.0087♣	♥16.7753♣	♥14.2118♣	♥7.5861♣
	(adaptive u^3,v^3,w^4)	ZZA	13.5620	10.5392	10.3465	19.6433	17.5977	15.9719
		ZZA_RDFX	12.9947	10.0199	9.9030	18.7144	16.7491	15.2775
	(no zig-zag functions u^3,v^3,w^4)	ZZA*	10.2076	7.8824	7.7516	14.7835	13.1858	12.0055
		HSDT_34X	10.1359	7.9003	7.7450	14.7167	13.1257	12.0035
	(no zig-zag functions u^4,v^4,w^3)	ZZA*_43X	10.2219	7.9368	7.7749	14.6905	13.1698	11.9624
	(general)	ZZA-XX	25.7514	20.0141	19.5885	37.1933	33.3160	30.2455
		ZZA-XX'	25.0131	19.4123	19.2121	36.2402	32.5449	29.5543

Table 5: Results of case a

Case a	Position	Exact	3-D FEA	Theories with similar results ♠	HRZZ	HRZZ4	MHR	MHR4	MHWZZA	MHWZZA4	MHR±	MHR4±
	up/min	-2.9889	-3.0036	-2.9343	-2.8735	-3.0613	-2.2894	-2.3466	-2.3467	-2.9941	-2.8906	-2.8280
u_α	down/max	1.2451	1.2439	1.2161	1.2228	1.3328	1.3072	1.2706	1.3399	1.2415	1.3941	1.5411
u_ζ	up/max	-	1.6049	1.5955	1.5575	1.6030	1.4770	1.4919	1.5413	1.5792	1.4692	1.4528
$x10^{-3}$	down/min	-	1.5365	1.5281	1.5575	1.5355	1.4228	1.4370	1.4749	1.5129	1.4221	1.4020
	up	2.5889	2.5207	2.5832	2.6382	2.6263	2.0558	2.1010	2.4924	2.5645	2.7942	1.9374
$\sigma_{\alpha\alpha}$	down/min	-24.9472	-24.9701	-24.9931	-25.3961	-25.9016	-25.7320	-27.5590	-24.0193	-25.0093	-30.3458	-23.7199
	max	22.3501	22.2540	22.3134	22.5404	23.2554	21.7952	21.4029	20.1360	22.8737	25.6642	17.4449
$\sigma_{\alpha\zeta}$	max	2.0000	2.0079	2.0000	2.0297	2.0162	2.0150	2.0131	1.9910	2.0075	2.2173	2.1705
$\sigma_{\zeta\zeta}$	up/max	-	1.0000	1.0000	1.0000	1.0000	1.0000	1.0000	1.0000	1.0000	1.0000	1.0000

Symbol ♠ indicates that theories ZZA, ZZA*, HWZZ, HWZZM, HWZZM*, ZZA-XX, ZZA-XX', ZZA_X_1 to ZZA_X_4, ZZA_RDFX, HWZZ_RDFX, ZZA*_43X, HSDT_34X obtain results which differ for less than 1%

Table 6: Results of case b

Case b	Position	3-D FEA	Theories with similar results ♠	HRZZ	HRZZ4	MHR	MHR4	MHWZZA	MHWZZA4	MHR±	MHR4±
u_α	up	-1.4225	-1.4259	-1.2851	-1.2737	-0.7871	-0.8028	-0.9253	-0.9346	-0.7871	-0.8028
$x10^{-2}$	down/max	3.0175	3.0345	2.7807	2.7522	1.0791	1.1007	2.2771	2.3001	1.0791	1.1007
	min	-3.1937	-3.1899	-2.9161	-2.8997	-2.3258	-2.3723	-2.6470	-2.6738	-2.3258	-2.3723
u_β	up	-0.4742	-0.4741	-0.4284	-0.4246	-0.2714	-0.2768	-0.3117	-0.3086	-0.2714	-0.2768
$x10^{-2}$	down/max	1.0059	1.0101	0.9269	0.9174	0.3905	0.3983	0.7669	0.7592	0.3905	0.3983
	min	-1.0646	-1.0610	-0.9720	-0.9666	-0.7588	-0.7740	-0.8912	-0.8822	-0.7588	-0.7740
	up	3.5705	3.5817	3.5238	3.2903	2.4225	1.9379	2.1422	2.1850	2.4225	1.9379
u_ζ	down	3.9477	3.9430	3.5238	3.5922	2.4515	2.7060	2.9220	2.9805	2.4515	2.7060
$x10^{-1}$	max	3.9543	3.9528	3.5238	3.5982	2.4515	2.7076	2.9272	2.9858	2.4515	2.7076
	min	3.5705	3.5817	3.5238	3.2902	2.4156	1.9379	2.1422	2.1850	2.4156	1.9379
	up/max	65.5801	65.4700	59.2481	58.7266	36.6356	37.3683	43.0362	42.6059	36.6356	37.3683
$\sigma_{\alpha\alpha}$	down	19.0188	19.0374	17.5260	17.3462	10.9241	11.1426	14.4979	14.3529	10.9241	11.1426
	min	-63.4908	-63.5153	-60.5002	-60.2204	-22.5919	-23.0437	-34.3783	-34.0345	-22.5919	-23.0437
	up	28.5252	28.5264	25.7727	25.5460	16.2212	16.5457	18.6913	18.5044	16.2212	16.5457
$\sigma_{\beta\beta}$	down/max	38.6704	38.6763	35.6350	35.2695	16.2723	16.5978	29.4769	29.1822	16.2723	16.5978
	min	-40.9643	-40.9541	-37.4025	-37.1924	-33.6573	-34.3305	-29.4958	-29.2009	-33.6573	-34.3305
	up/min	-13.8956	-13.9000	-12.5533	-12.4427	-7.8211	-7.9775	-9.1325	-9.2238	-7.8211	-7.9775
$\sigma_{\alpha\beta}$	down	7.3693	7.3791	6.7909	6.7212	2.1139	2.1562	5.6179	5.6741	2.1139	2.1562
	max	13.4573	13.4609	12.8242	12.7650	4.1559	4.2390	7.2741	7.3469	4.1559	4.2390
$\sigma_{\alpha\zeta}$	max	22.5907	22.4046	19.7134	19.4974	20.3905	22.4648	21.9681	21.9681	20.3905	22.4648
	min	-10.4100	-10.1051	-9.3251	-9.2209	-0.3555	-5.1433	-10.2517	-10.2497	-0.3555	-5.1433
$\sigma_{\beta\zeta}$	max	7.4682	7.4796	6.5711	6.4991	6.5250	6.4090	5.3118	5.3649	6.5250	6.4090
	min	-3.3684	-3.3567	-3.1084	-3.0736	-0.1138	-1.4673	-2.6080	-2.6341	-0.1138	-1.4673
$\sigma_{\zeta\zeta}$	up/max	1.0000	1.0000	1.0000	1.0000	1.0000	1.0000	1.0000	1.0000	1.0000	1.0000
	min	-1.1414	-1.1359	-1.0101	-0.9963	-0.0069	-0.3866	-1.5002	-1.4852	-0.0069	-0.3866

Symbol ♠ indicates that theories ZZA, ZZA*, HWZZ, HWZZM, HWZZM*, ZZA-XX, ZZA-XX', ZZA_X_1 to ZZA_X_4, ZZA_RDFX, HWZZ_RDFX, ZZA*_43X, HSDT_34X obtain results which differ for less than 1%

Table 7: Results of case c

Case c	Position	3-D FEA	Theories with similar results ♠	HRZZ	HRZZ4	MHR	MHR4	MHWZZA	MHWZZA4	MHR±	MHR4±
u_α	up	-0.3828	-0.3866	-0.3848	-0.3689	-0.3702	-0.3753	-0.3834	-0.3828	-0.3296	-0.3304
$x10^{-2}$	down/max	4.6261	4.6723	4.8664	4.5824	4.7763	4.9984	4.6581	4.6412	4.1652	3.9997
	min	-0.3828	-0.3866	-0.3848	-0.3689	-0.3702	-0.3753	-0.3834	-0.3828	-0.3296	-0.3304
u_β	up/min	-0.0443	-0.0444	-0.0441	-0.0430	-0.0546	-0.0541	-0.0429	-0.0439	-0.0518	-0.0508
$x10^{-1}$	down	1.0694	1.0712	1.0981	1.0499	0.7792	0.7856	1.0772	1.0726	0.7420	0.7045
	max	0.1059	0.1046	0.1087	0.1040	0.0754	0.0761	0.1050	0.1046	0.7420	0.7045
u_ς	up	0.9619	0.9613	0.9683	0.9677	0.0927	0.0930	0.9649	0.9618	0.9431	0.9556
$x10^{-1}$	down/min	0.8307	0.8306	0.9683	0.8113	0.7956	0.7649	0.8332	0.8308	0.8103	0.7508
	max	0.9623	0.9620	0.9683	0.9681	0.9276	0.9324	0.9654	0.9622	0.9434	0.9558
	up/max	32.8699	32.8733	33.0394	31.6808	31.9053	32.3405	32.9073	32.8665	35.4284	35.5056
$\sigma_{\alpha\alpha}$	down	0.6546	0.6512	0.6156	0.6234	-0.2182	-0.3109	0.6628	0.6585	-0.5368	-0.5376
	min	-29.9808	-29.9958	-30.0560	-27.3284	-26.0877	-26.4964	-30.1572	-29.9846	-32.9355	-32.9490
	up	1.8425	1.8367	1.8369	1.7880	2.1963	2.1852	1.7960	1.8299	2.1387	2.1065
$\sigma_{\beta\beta}$	down	3.3715	3.3631	3.4948	3.3219	2.8462	2.9200	3.3974	3.3838	2.8904	2.7598
	max	3.3715	3.3631	3.4948	3.3219	2.8462	2.9200	3.3974	3.3838	2.8873	2.7570
	min	-1.3314	-1.3317	-1.3498	-1.1916	-0.9822	-0.9649	-1.3887	-1.3439	-1.1399	-1.2403
	up	-1.3986	-1.4076	-1.3983	-1.3537	-1.5513	-1.5524	-1.3761	-1.3923	-1.5757	-1.5609
$\sigma_{\alpha\beta}$	down	0.2595	0.2573	0.2684	0.2555	0.2130	0.2178	0.2179	0.2180	0.2138	0.2040
	max	1.1126	1.1202	1.1228	1.0038	0.8944	0.9214	0.9214	0.9214	1.0614	1.0802
	min	-1.3986	-1.4076	-1.3983	-1.3537	-1.5513	-1.5524	-1.5522	-1.5526	-1.5757	-1.5609
$\sigma_{\alpha\varsigma}$	max	11.1897	11.1938	10.8151	10.9233	10.1734	9.7946	10.6435	11.1353	10.2751	10.0958
	min	-0.2687	-0.2697	-0.4964	-0.5014	0	0	-0.1740	-0.9738	0	0
$\sigma_{\beta\varsigma}$	max	1.1471	1.1381	1.1243	0.9280	1.6464	1.5236	1.1096	1.1430	1.5425	1.3516
	min	-1.9038	-1.9038	-1.9937	-1.9431	-1.6117	-1.6532	-1.9259	-1.9181	-1.6381	-1.5689
$\sigma_{\varsigma\varsigma}$	up/max	1.0000	1.0000	1.0000	1.0000	1.0000	1.0000	1.0000	1.0000	1.0000	1.0000
	min	-0.3524	-0.3530	-0.3253	-0.2348	-0.0860	-0.0795	-0.3509	-0.3501	-0.0666	-0.0630

Symbol ♠ indicates that theories ZZA, ZZA*, HWZZ, HWZZM, HWZZM*, ZZA-XX, ZZA-XX', ZZA_X_1 to ZZA_X_4, ZZA_RDFX, HWZZ_RDFX, ZZA*_43X, HSDT_34X obtain results which differ for less than 1%

Table 8: Results of case d

Case d	Position	3-D FEA	Theories with similar results ♠	HRZZ	HRZZ4	MHR	MHR4	MHWZZA	MHWZZA4	MHR±	MHR4±
	up	-3.3669	-3.4009	-3.5729	-3.5752	-0.2244	-0.2249	-2.1659	-2.7108	-3.1352	-3.0571
u_α	down	3.2057	3.2381	3.1356	3.1303	0.2540	0.2687	1.9001	2.3008	3.1616	3.0203
$x10^{-5}$	max	5.8215	5.8803	5.8864	5.8848	0.2540	0.2687	5.0927	4.9530	5.0817	4.9526
	min	-5.0845	-5.1359	-5.1855	-5.1852	-0.2244	-0.2249	-3.4330	-4.2801	-5.0637	-4.8584
	up	3.1748	3.1759	2.7584	3.2161	0.0260	0.1518	2.6772	2.5937	2.6652	2.6037
u_ς	down	2.8319	2.8297	2.7584	2.8374	0.0246	0.1518	2.2484	2.2037	2.6697	2.5342
$x10^{-4}$	max	3.1786	3.1809	2.7584	3.2207	0.0260	0.1518	2.6806	2.5963	2.6723	2.6104
	min	2.8164	2.8224	2.7584	2.8224	0.0246	0.1514	2.2254	2.1911	2.6514	2.5342
	up	0.2687	0.2673	0.4489	0.4534	0.0343	0.0342	0.2765	0.3404	0.3857	0.3761
$\sigma_{\alpha\alpha}$	down	-0.3953	-0.3928	-0.3909	-0.3948	-0.0343	-0.0343	-0.2577	-0.2811	-0.3929	-0.3755
	max	3.2945	3.2939	3.5599	3.5955	0.4449	0.4469	2.6611	3.2268	3.2550	3.1707
	min	-3.2789	-3.2801	-3.9846	-4.0245	-0.5511	-0.5569	-4.0573	-3.6558	-3.3314	-3.2136
$\sigma_{\alpha\varsigma}$	max	8.0017	8.0101	7.0558	7.0412	2.7754	2.5602	10.2099	7.1725	5.8578	5.5192
$\sigma_{\varsigma\varsigma}$	up/max	1.0000	1.0000	1.0000	1.0000	1.0000	1.0000	1.0000	1.0000	1.0000	1.0000

Symbol ♠ indicates that theories ZZA, ZZA*, HWZZ, HWZZM, HWZZM*, ZZA-XX, ZZA-XX', ZZA_X_1 to ZZA_X_4, ZZA_RDFX, HWZZ_RDFX, ZZA*_43X, HSDT_34X obtain results which differ for less than 1%

Table 9: Results of case e

Case e	Position	3-D FEA	Theories with similar results ♠	HRZZ	HRZZ4	MHR	MHR4	MHWZZA	MHWZZA4	MHR±	MHR4±
	up	-1.8968	-1.8969	-1.7534	-1.7747	-0.7300	-0.7065	-1.6350	-2.0760	-0.4696	-0.6809
u_α	down	1.1906	1.1907	1.1127	1.1170	1.4200	1.5136	2.1954	1.5541	0.5854	0.3130
$x10^{-3}$	max	2.1563	2.1564	1.8550	1.8548	1.4200	1.5136	2.1954	1.8856	0.5854	1.2200
(x=0)	min	-1.8968	-1.8969	-1.7534	-1.7747	-0.7300	-0.7065	-2.9024	-2.0760	-0.4696	-0.6809
	up	2.2932	2.2935	1.9792	2.1845	2.6016	1.5179	2.8767	2.6884	3.4067	8.1597
u_ς	down	1.5017	1.5010	1.9792	1.4565	2.4642	1.5176	2.1452	1.9513	3.8215	1.9934
$x10^{-2}$	max	2.2932	2.2935	1.9792	2.1845	2.6016	1.5182	2.8769	2.6885	3.8215	8.1666
(x=Lx/4)	min	1.5005	1.5005	1.9792	1.4558	2.4642	1.5144	1.7926	1.9513	2.7925	1.8886
	up	0.1610	0.1611	0.1771	0.1789	4.1485	4.0898	0.2458	0.2382	0.0492	0.0713
$\sigma_{\alpha\alpha}$	down	-0.1588	-0.1589	-0.1118	-0.1129	-4.0382	-4.0905	-0.1743	-0.1627	-0.0821	-0.0536
(x=Lx/4)	max	3.8411	3.8430	3.7779	3.8157	4.1485	4.0898	5.5363	5.3926	1.3409	1.8016
	min	-3.8574	-3.8545	-3.5324	-3.5677	-4.0382	-4.0905	-4.4724	-4.0529	-1.7132	-0.9363
$\sigma_{\alpha\varsigma}$ (x=0)	max	3.1473	3.1430	2.2743	2.2621	2.6035	2.6281	2.8874	2.7631	1.2548	1.1693
$\sigma_{\varsigma\varsigma}$ (x=Lx/4)	up/max	1.0000	1.0000	1.0000	1.0000	1.0000	1.0000	1.0000	1.0000	1.0000	1.0000

Symbol ♠ indicates that theories ZZA, ZZA*, HWZZ, HWZZM, HWZZM*, ZZA-XX, ZZA-XX', ZZA_X_1 to ZZA_X_4, ZZA_RDFX, HWZZ_RDFX, ZZA*_43X, HSDT_34X obtain results which differ for less than 1%

Table 10: Results for case f

Case f	Position	3-D FEA	Theories with similar results ♠	HRZZ	HRZZ4	MHR	MHR4	MHWZZA	MHWZZA4	MHR±	MHR4±
	up	2.1201	2.1208	2.1205	2.1169	-2.0074	-2.0003	-1.7381	-1.7409	-2.0074	-2.0003
u_α	down	-2.4786	-2.4784	-2.4781	-2.4777	0.3235	0.3339	1.2823	1.2989	0.3235	0.3339
$x10^{-2}$	max	2.1201	2.1208	2.1205	2.1169	1.6115	1.6643	1.9011	1.9110	1.6115	1.6643
	min	-2.4786	-2.4784	-2.4781	-2.4777	-2.4788	-2.4971	-2.0871	-2.0836	-2.4788	-2.4971
	up	7.7178	7.7177	0	7.4874	8.0429	8.0488	7.6008	7.6008	8.0429	8.0488
u_ζ	down/min	0	0	0	0	0	0	0	0	0	0
$x10^{-3}$	max	7.7446	7.7499	0	7.4934	8.1313	8.1420	7.6008	7.6203	8.1313	8.1420
	up	0.1357	0.1348	0.1106	0.1061	0.2579	0.2547	0.2903	0.2898	0.2579	0.2547
$\sigma_{\alpha\alpha}$	down/min	-0.2849	-0.2845	-0.3069	-0.3112	-0.3834	-0.3811	-0.2738	-0.2705	-0.3834	-0.3811
	max	0.1357	0.1348	0.1775	0.1783	0.2579	0.2547	0.2903	0.2898	0.2579	0.2547
$\sigma_{\alpha\zeta}$	min	-0.5213	-0.5108	-0.5014	-0.4964	-0.4895	-0.4884	-0.5175	-0.5148	-0.4895	-0.4884
$\sigma_{\zeta\zeta}$	up/max	1.0000	1.0000	1.0000	1.0000	1.0000	1.0000	1.0000	1.0000	1.0000	1.0000
	min	0	0	0	0	0	0	0	0	0	0

Symbol ♠ indicates that theories ZZA, ZZA*, HWZZ, HWZZM, HWZZM*, ZZA-XX, ZZA-XX', ZZA_X_1 to ZZA_X_4, ZZA_RDFX, HWZZ_RDFX, ZZA*_43X, HSDT_34X obtain results which differ for less than 1%

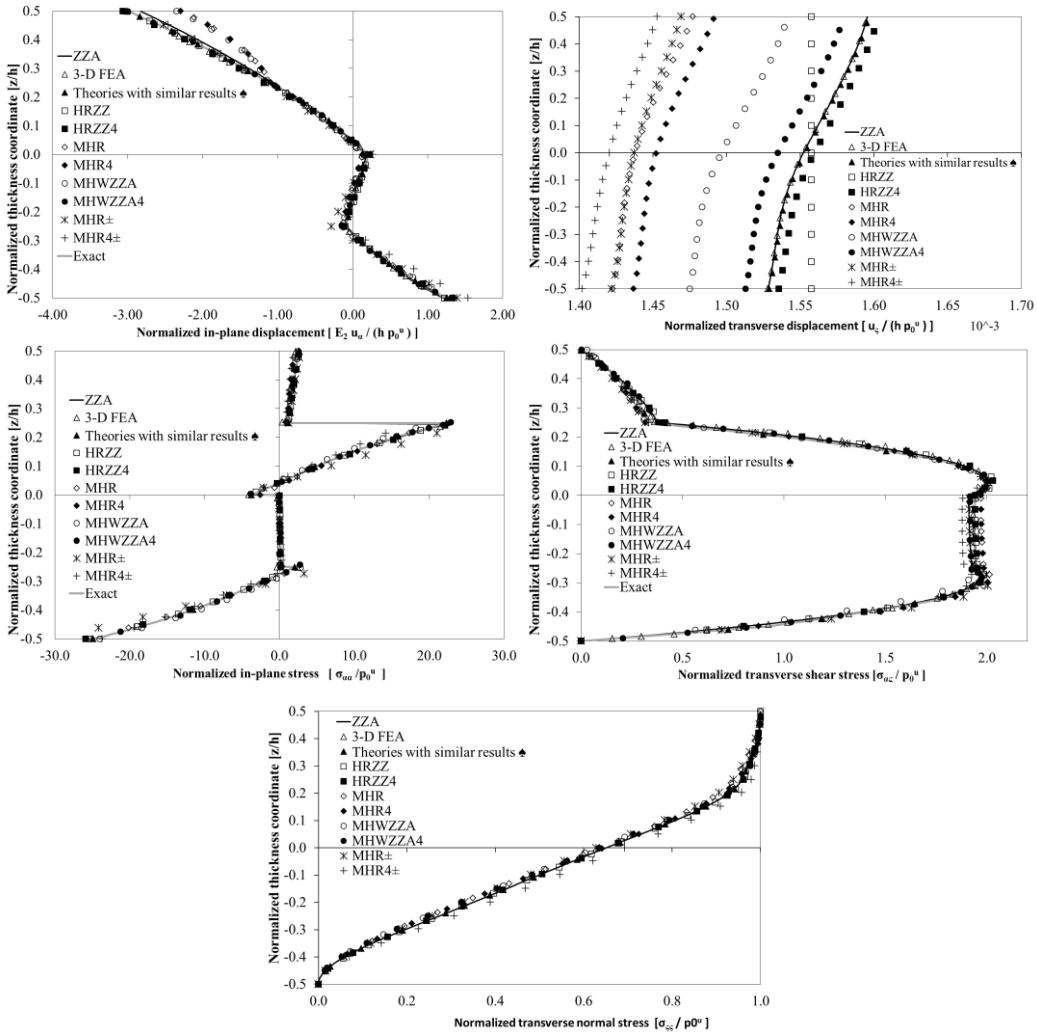

Figure 1: Results of case a; Symbol ♠ indicates that theories ZZA, ZZA*, HWZZ, HWZZM, HWZZM*, ZZA-XX, ZZA-XX', ZZA_X_1 to ZZA_X_4, ZZA_RDFX, HWZZ_RDFX, ZZA*_43X, HSDT_34X obtain results which differ for less than 1%

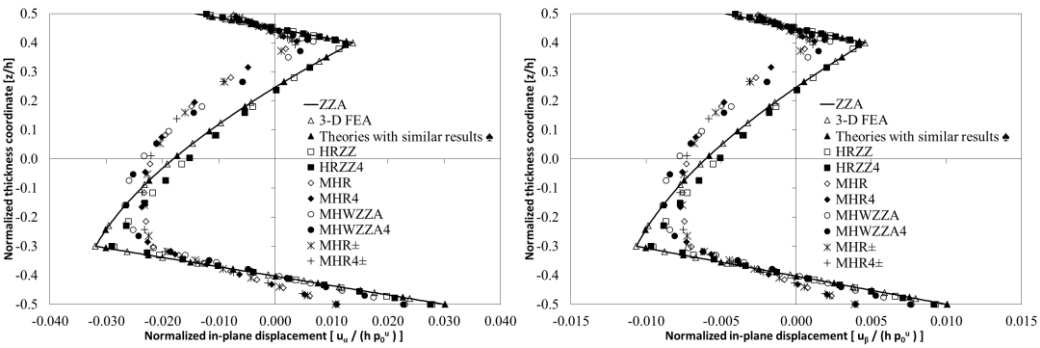

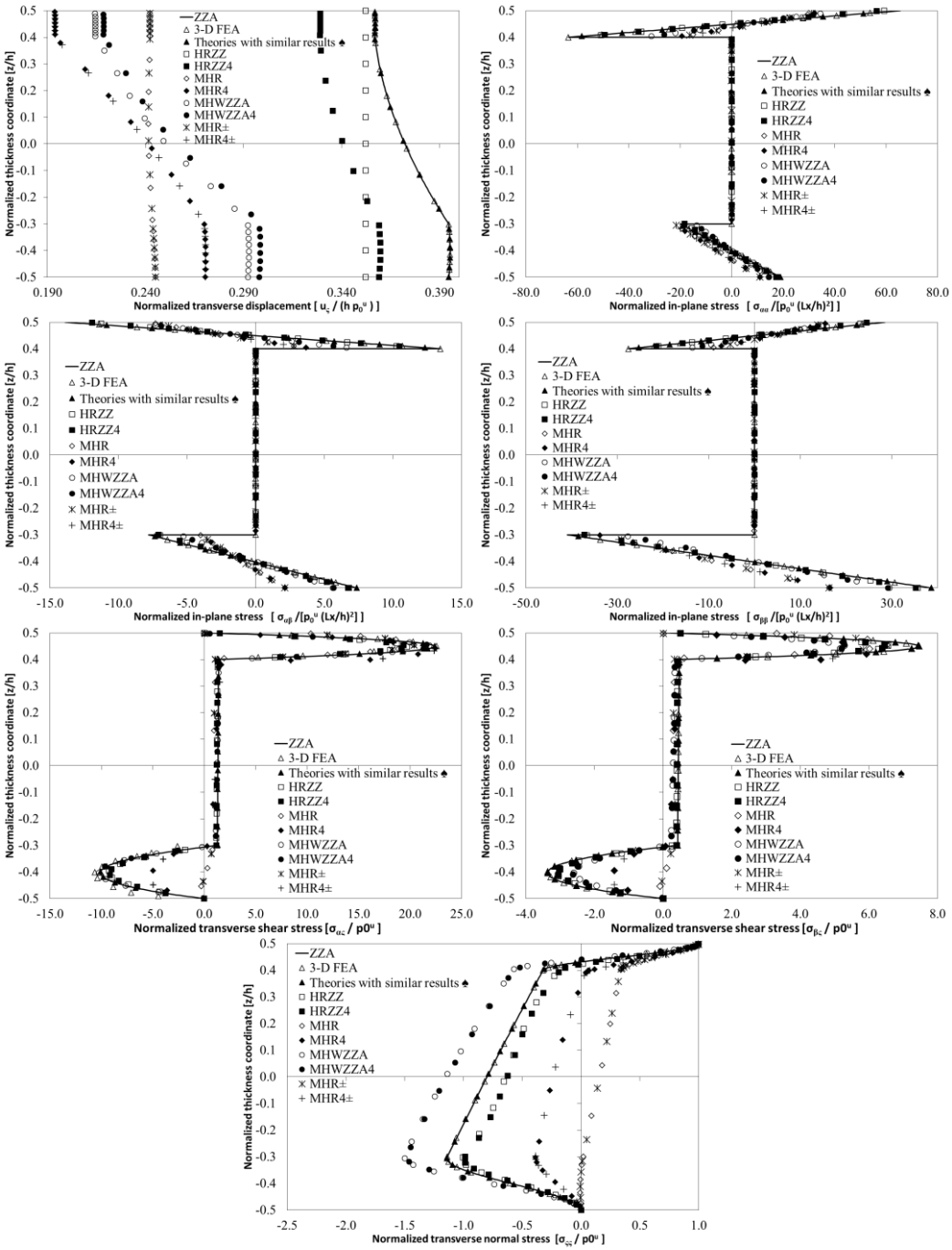

Figure 2: Results of case b; Symbol ♠ indicates that theories ZZA, ZZA*, HWZZ, HWZZM, HWZZM*, ZZA-XX, ZZA-XX', ZZA_X_1 to ZZA_X_4, ZZA_RDFX, HWZZ_RDFX, ZZA*_43X, HSDT_34X obtain results which differ for less than 1%

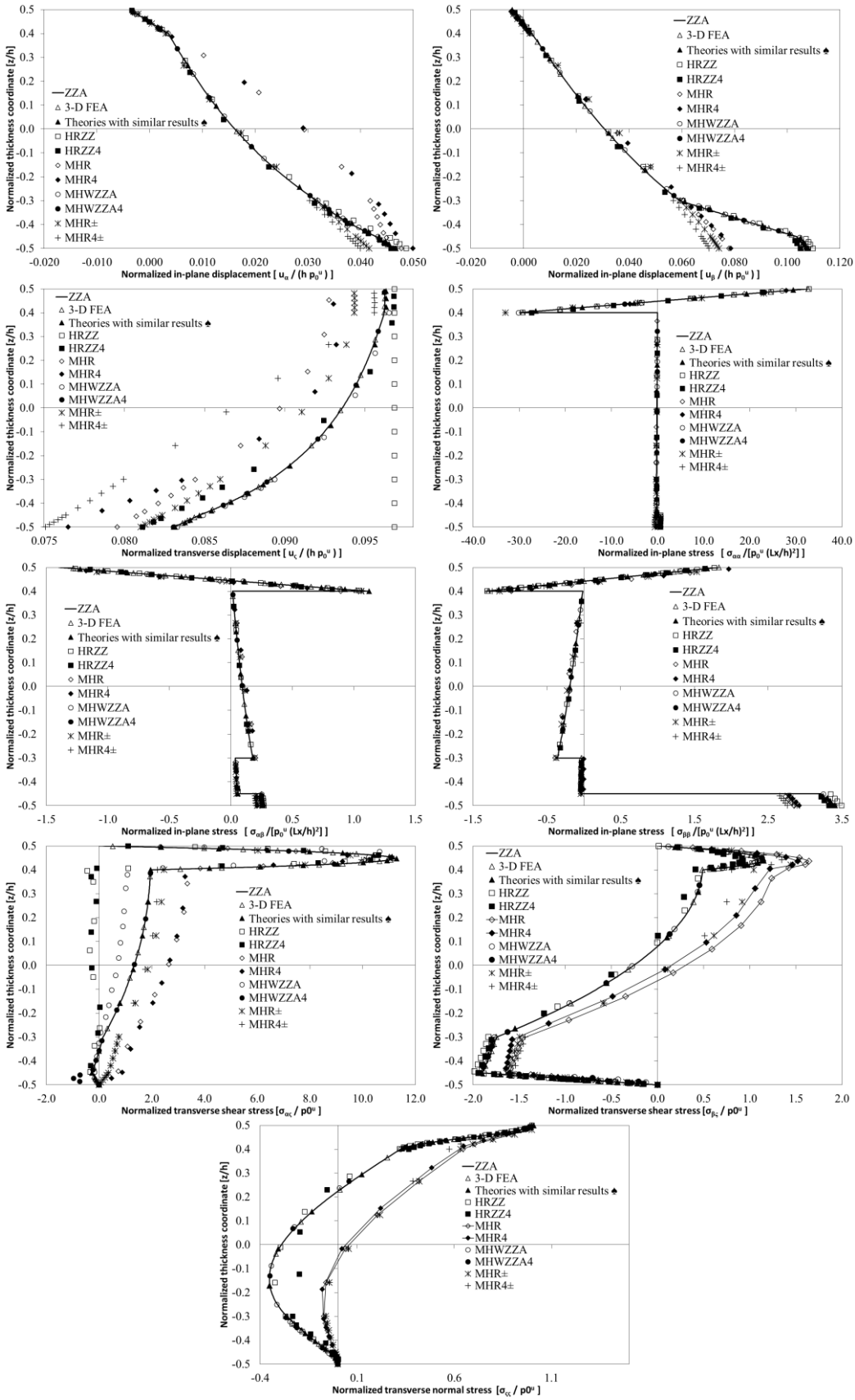

Figure 3: Results of case c; Symbol ♠ indicates that theories ZZA, ZZA*, HWZZ, HWZZM, HWZZM*, ZZA-XX, ZZA-XX', ZZA_X_1 to ZZA_X_4, ZZA_RDFX, HWZZ_RDFX, ZZA*_43X, HSDT_34X obtain results which differ for less than 1%

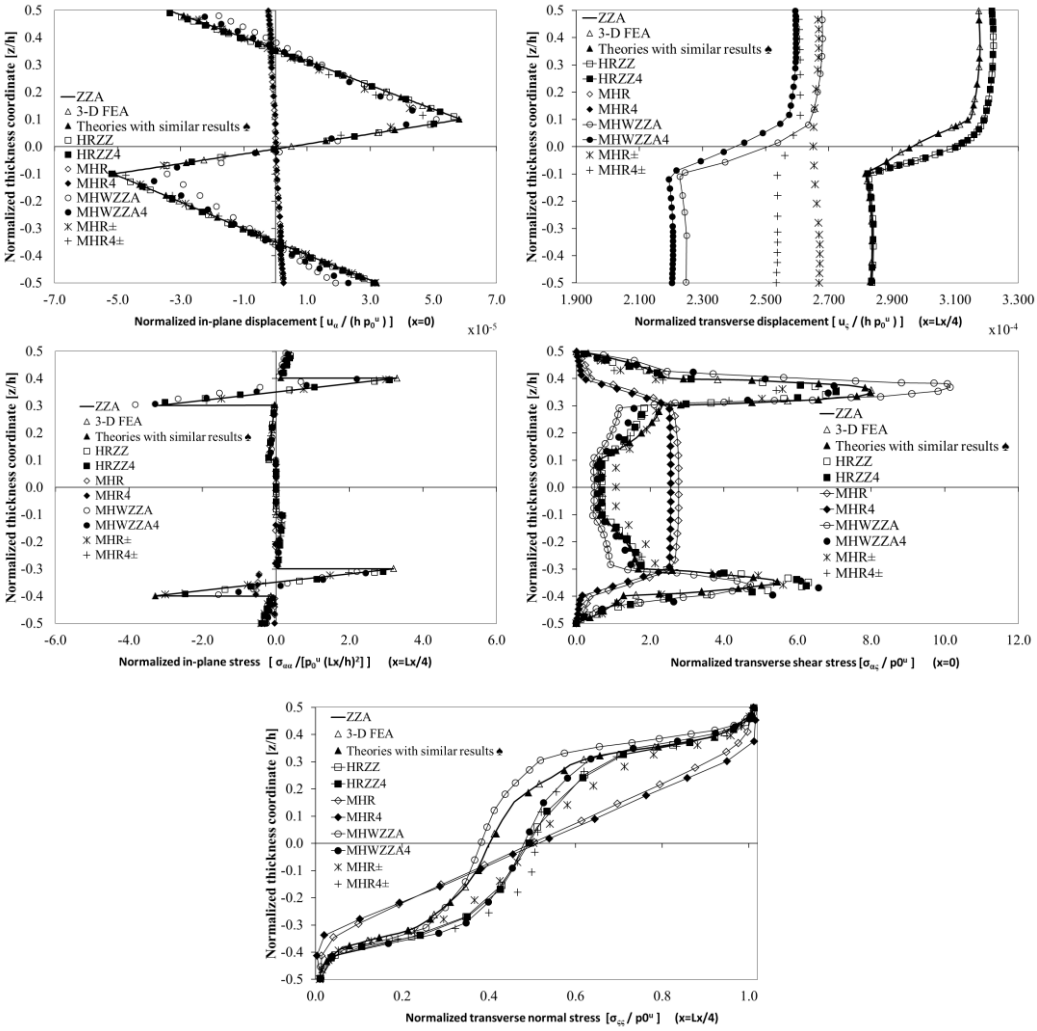

Figure 4: Results of case d; Symbol ♠ indicates that theories ZZA, ZZA*, HWZZ, HWZZM, HWZZM*, ZZA-XX, ZZA-XX', ZZA_X_1 to ZZA_X_4, ZZA_RDFX, HWZZ_RDFX, ZZA*_43X, HSDT_34X obtain results which differ for less than 1%

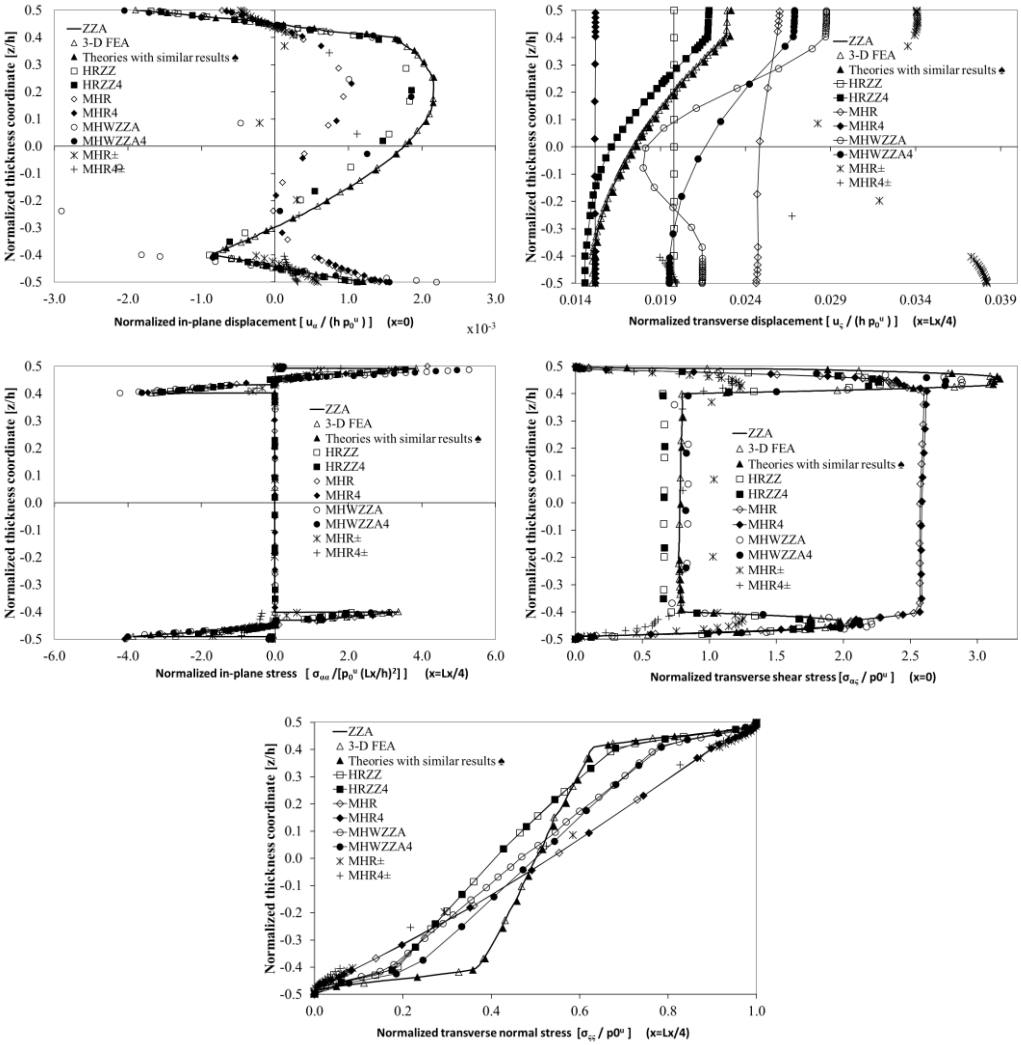

Figure 5: Results of case e; Symbol ♠ indicates that theories ZZA, ZZA*, HWZZ, HWZZM, HWZZM*, ZZA-XX, ZZA-XX', ZZA_X_1 to ZZA_X_4, ZZA_RDFX, HWZZ_RDFX, ZZA*_43X, HSDT_34X obtain results which differ for less than 1%

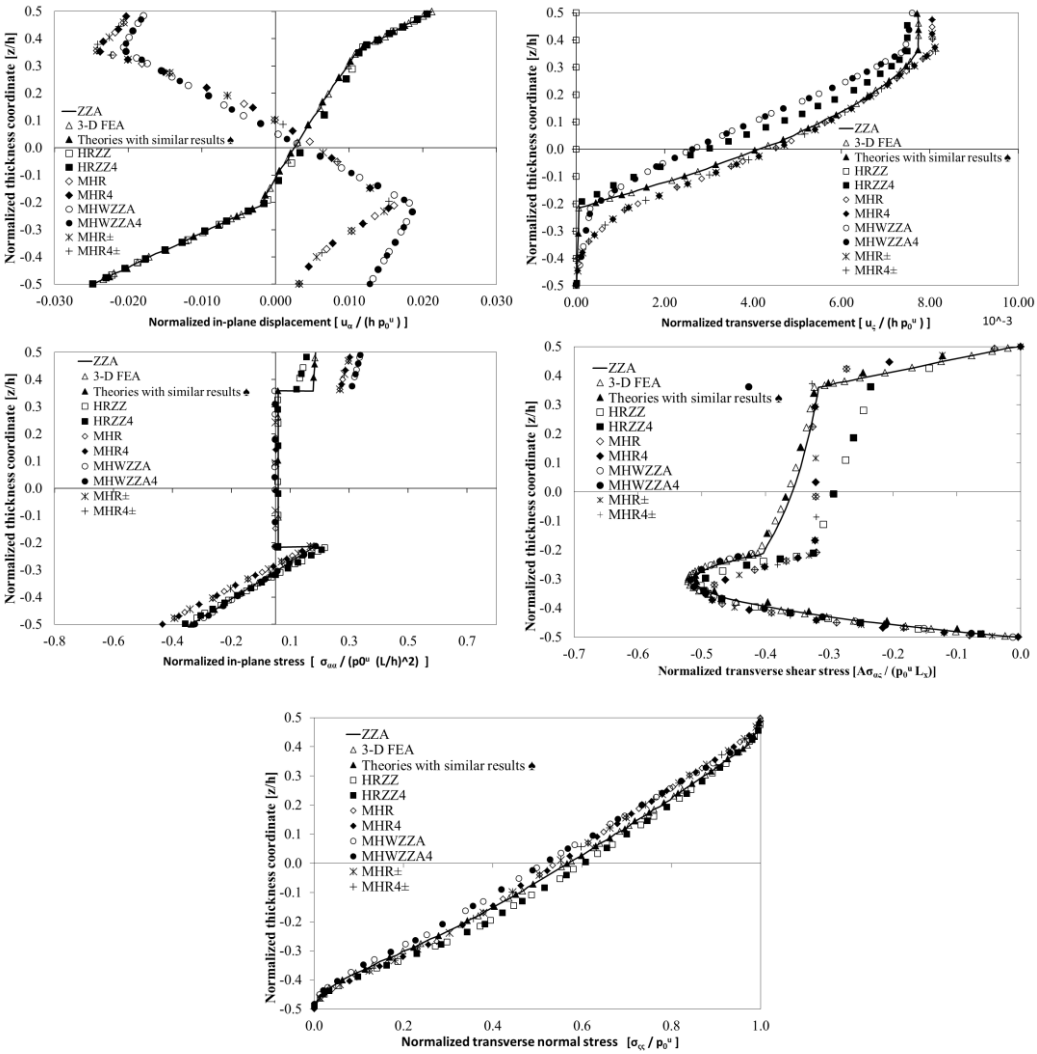

Figure 6: Results of case f; Symbol ♠ indicates that theories ZZA, ZZA*, HWZZ, HWZZM, HWZZM*, ZZA-XX, ZZA-XX', ZZA_X_1 to ZZA_X_4, ZZA_RDFX, HWZZ_RDFX, ZZA*_43X, HSDT_34X obtain results which differ for less than 1%